NOAA Technical Report ERL 368-MESA 5

Analysis of Current Meter Observations in the New York Bight Apex August 1973–June 1974

Richard C. Patchen
Elmo E. Long
Bruce B. Parker

Prepared for the MESA New York Bight Project
by the National Ocean Survey, NOAA

June 1976

U.S. DEPARTMENT OF COMMERCE
National Oceanic and Atmospheric Administration
Environmental Research Laboratories

NOAA Technical Report ERL 368-MESA 5

Analysis of Current Meter Observations in the New York Bight Apex August 1973–June 1974

Richard C. Patchen
Elmo E. Long
Bruce B. Parker

Prepared for the MESA New York Bight Project
by the Office of Marine Surveys and Maps
Oceanographic Division
Oceanographic Surveys Branch
National Ocean Survey
Rockville, Md.

June 1976

U.S. DEPARTMENT OF COMMERCE
Elliot Richardson, Secretary

National Oceanic and Atmospheric Administration
Robert M. White, Administrator

Environmental Research Laboratories
Wilmot Hess, Director

National Ocean Survey
Allen L. Powell, Director

BOULDER, COLORADO

NOTICE

The Environmental Research Laboratories do not approve, recommend, or endorse any proprietary product or proprietary material mentioned in this publication. No reference shall be made to the Environmental Research Laboratories or to this publication furnished by the Environmental Research Laboratories in any advertising or sales promotion which would indicate or imply that the Environmental Research Laboratories approve, recommend, or endorse any proprietary product or proprietary material mentioned herein, or which has as its purpose an intent to cause directly or indirectly the advertised product to be used or purchased because of this Environmental Research Laboratories publication.

CONTENTS

ANALYSIS OF CURRENT METER OBSERVATIONS IN THE NEW YORK BIGHT APEX AUGUST 1973 — JUNE 1974

Richard C. Patchen
Elmo E. Long
Bruce B. Parker

1. INTRODUCTION

The Marine Ecosystems Analysis (MESA) Program New York Bight Project of the National Oceanic and Atmospheric Administration's (NOAA) Environmental Research Laboratories (ERL) is a multidisciplinary research field program designed to describe the oceanographic processes of the New York Bight fully. To establish the significant temporal and spatial scales and to understand the dynamics of the water movement in the New York Bight, a comprehensive physical oceanographic program was undertaken. Water movement, which is the principal transport mechanism affecting biological, chemical, and geological distributions, can be described utilizing current meter observations, wind observations, tide records, and water column samples. A complete description of the circulation of the New York Bight is an essential input into the decision-making processes of the mariner, legislator, environmentalist and the recreational community developer.

The primary oceanographic mission of NOAA's National Ocean Survey (NOS) is the acquisition, interpretation, and dissemination of oceanographic information, particularly information relating to tide and tidal current regimes of estuaries and nearshore regions. In response to present environmental and energy related issues, NOAA is expanding its capabilities and expertise. The Oceanographic Surveys Branch within NOS is a major participant in the MESA Project, working with the Physical Oceanography Laboratory (PhOL) of ERL's Atlantic Oceanographic and Meteorological Laboratories (AOML) to determine the total hydrodynamic system of the New York Bight.

2. FIELD PROGRAM

The major emphasis for the first stage of the MESA Project was a description of the water movement within the New York Bight in the region commonly called the apex of the bight, defined by an approximate 50-km square area extending seaward from the mouth of the Hudson Estuary. Relatively few historical observations are available which allow any insight into the spatial and temporal scales of motion. Charnell and Hansen (1974) gave a complete account of the oceanographic knowledge in the apex region before the present survey.

A comprehensive field program in the apex region was designed to resolve the temporal and spatial scales of the water movement. To determine the overall circulation in the late summer and fall, 13 stations were deployed in 1973; to gather information relating to the spatial resolution and seasonal variation, two transects were maintained

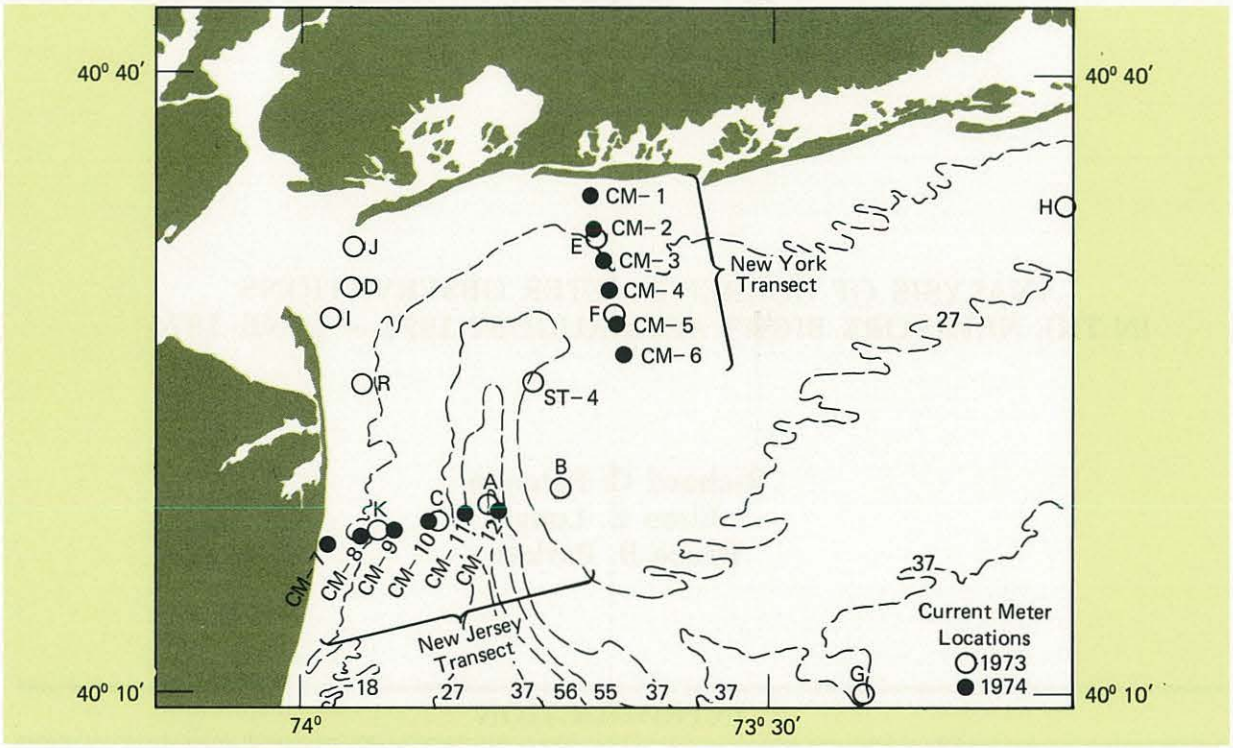

Figure 1. Current meter station locations for observations obtained from August 1973 to June 1974 in the New York Bight Apex.

in the spring of 1974. Each transect determines an outer boundary of the apex region and contains six stations. Figure 1 illustrates the station locations for the 1973 and 1974 observations. Stations CM-1 through CM-12 were maintained into September 1974, but analyses of those observations are not included in this report. Aanderaa current meter models RCM-4 and RCM-5, which measure current speed and direction utilizing a 10-min sampling rate, were used throughout the survey. The current meters were deployed using a taut-line mooring system. Table 1 gives current meter locations and periods of observations. Current meters were calibrated at the Mobile Calibration Laboratory, located at Floyd Bennett Field, Brooklyn, N.Y., after each field season; Table 2 describes the current meter specifications for the Aanderaa systems.

3. DATA PROCESSING

Within NOS's Office of Marine Surveys and Maps, the Oceanographic Division's Oceanographic Surveys Branch has primary responsibility for the processing and data analysis of current meter information. After deployment and recovery of the current meters used in the MESA Project, data tapes from the current meters were "transcribed" (translated to a computer readable format). All raw data tapes for which timing could be accurately determined were then edited for erroneous values of speed and direction, resulting from meter malfunction, without utilizing any filtering techniques and preserving the 10-min samples.

Table 1 indicates which data tapes had recoverable (RC), partly recoverable (PRC), or unrecoverable (URC) timing and which were edited. Edited raw data tapes were sent to the National Oceanographic Data Center (NODC) of the Environmental Data Service (EDS) for public dissemination and archival of the data and to PhOL-AOML for analysis. Charnell and Mayer (1975) described their interpretation of the first phase of these data.

Station No.	Latitude Longitude	Observation Information: Dates of Observations	Observation Information: Charted Depth (Meters)	Observation Information: Depth of Meter Above Bottom (Meters)	Stage of Processing: Data Quality RC, PRC or URC	Stage of Processing: Data Edited	Stage of Processing: Data Sent to NODC	Standard Analysis: Harmonic	Standard Analysis: Rotary Reduction	Standard Analysis: Tidal Current Ellipses	Standard Analysis: Time Series Analysis
A	40°19.4′N 73°47.8′W	8/23-10/9 73	45.11	25.1	RC	●	●	●	●	●	●
				14.9	RC	●	●		●		
				8.8	RC	●	●	●	●	●	●
				0.5	URC						
	40°19.2′N 73°48.0′W	10/23-12/10 73	46.02	25.2	URC						
				14.9	RC	●	●	●	●	●	●
				8.8	RC	●	●	●	●	●	●
				1.0	RC	●	●	●	●	●	●
B	40°20.0′N 73°43.5′W	8/23 10/9 73	24.69	8.9	RC	●	●	●	●	●	●
				0.4	URC						
	40°20.0′N 73°43.0′W	10/23-12/10 73	24.69	8.9	URC						
				1.0	URC						
C	40°18.4′N 73°51.5′W	8/23-10/9 73	24.38	8.3	RC	●	●	●	●	●	●
				2.7	RC	●	●	●	●	●	●
	40°18.4′N 73°50.9′W	10/23-12/10 73	24.69	8.9	RC	●	●	●	●	●	●
				2.8	URC						
D	40°29.7′N 73°56.7′W	8/30-10/9 73	9.75	0.5	RC	●	●	●	●	●	●
	40°29.7′N 73°56.6′W	10/24-12/7 73	11.89	1.0	RC	●	●	●	●	●	●
E	40°32.0′N 73°40.9′W	8/31-10/11 73	16.76	7.6	RC	●	●	●	●	●	●
				7.6	URC						
	40°32.0′N 73°41.0′W	10/24-12/10 73	16.76	2.7	RC	●	●	●	●	●	●
F	40°28.2′N 73°40.0′W	8/31-10/11 73	21.95	8.8	RC	●	●	●	●	●	●
				0.5	RC	●	●	●	●	●	●
	40°28.4′N 73°40.0′W	10/23-12/16 73	22.56	8.8	RC	●	●	●	●	●	●
				1.0	RC	●	●	●	●	●	●

Table 1. Current Meter Information (Composite Table Containing Information Relating to Data Observed, Processing Completed, and Standard Analysis Performed.)

Station No.	Latitude Longitude	Observation Information			Stage of Processing			Standard Analysis			
		Dates of Observations	Charted Depth (Meters)	Depth of Meter Above Bottom (Meters)	Data Quality RC, PRC or URC	Data Edited	Data Sent to NODC	Harmonic	Rotary Reduction	Tidal Current Ellipses	Time Series Analysis
G	40°10.2'N 73°24.8'W	8/31-10/11 73	36.58	21.3 15.2 9.1 3.0	URC RC URC RC	● ● ● ●	● ● ● ●	● ● ● ●	● ● ● ●	● ● ● ●	● ● ● ●
H	40°33.4'N 73°10.6'W	10/4-10/10 73	24.69	8.8 0.5	RC RC	● ●	● ●	● ●	● ●	● ●	● ●
I	40°28.1'N 73°58.0'W	10/24-12/6 73	6.10	1.2	PRC	●	●		●		●
J	40°31.6'N 73°56.6'W	10/24-12/7 73	7.01	0.9	PRC	●	●		●		●
K	40°18.0'N 73°55.0'W	10/23-12/10 73	20.12	8.8 1.0	RC RC	● ●	● ●	● ●	● ●	● ●	● ●
R	40°25.0'N 73°56.0'W	11/11-12/7 73	14.33	1.0	RC	●	●	●	●	●	●
ST-4	40°25.0'N 73°45.1'W	9/24-10/11 73	27.43	11.2 2.7	RC RC	● ●	● ●	● ●	● ●	● ●	● ●
CM-1	40°34.0'N 73°41.5'W	4/24-6/24 74	10.67	1.5	RC	●	●	●	●	●	●
CM-2	40°32.5'N 73°41.2'W	4/24-6/24 74	16.15	1.2 6.7	RC RC	● ●	● ●	● ●	● ●	● ●	● ●
CM-3	40°31.0'N 73°40.7'W	4/23-6/24 74	17.98	1.5 8.5	RC RC	● ●	● ●	● ●	● ●	● ●	● ●
CM-4	40°29.5'N 73°40.3'W	4/23-6/24 74	18.59	3.7 10.7	RC RC	● ●	● ●	● ●	● ●	● ●	● ●
CM-5	40°28.0'N 73°39.8'W	4/24-6/24 74	22.86	1.5 6.7 13.7	RC RC RC	● ● ●	● ● ●	● ● ●	● ● ●	● ● ●	● ● ●
CM-6	40°26.5'N 73°39.4'W	5/22-6/24 74	21.95	1.5 6.7 13.7	RC RC RC	● ● ●	● ● ●	● ● ●	● ● ●	● ● ●	● ● ●

Table 1. Continued.

Station No.	Latitude Longitude	Observation Information: Dates of Observations	Observation Information: Charted Depth (Meters)	Observation Information: Depth of Meter Above Bottom (Meters)	Stage of Processing: Data Quality RC, PRC or URC	Stage of Processing: Data Edited	Stage of Processing: Data Sent to NODC	Standard Analysis: Harmonic	Standard Analysis: Rotary Reduction	Standard Analysis: Tidal Current Ellipses	Standard Analysis: Time Series Analysis
CM-7	40°17.3'N 73°58.2'W	4/1-5/14 74	10.06	1.5	RC	●	●	●	●	●	●
		5/14-6/26 74		1.5	URC						
CM-8	40°17.7'N 73°56.0'W	4/1-5/15 74	18.59	4.0	RC	●	●	●	●	●	●
				10.7	RC	●	●	●	●	●	●
		5/14-6/26 74		4.0	URC						
				10.7	URC						
CM-9	40°18.0'N 73°54.0'W	4/1-5/28 74	21.03	6.7	RC	●	●	●	●	●	●
				13.7	RC	●	●	●	●	●	●
		5/28-6/26 74		6.7	RC	●	●	●	●	●	●
				13.7	RC	●	●	●	●	●	●
CM-10	40°18.4'N 73°51.6'W	4/8-5/28 74	23.47	1.5	RC	●	●	●	●	●	●
				8.8	URC						
				15.2	RC	●	●	●	●	●	●
		5/28-6/27 74		1.5	URC						
				8.8	RC	●	●	●	●	●	●
				15.2	RC	●	●	●	●	●	●
CM-11	40°18.6'N 73°50.1'W	4/8-6/4 74	32.92	1.2	URC						
				11.6	URC						
				18.9	RC	●	●	●	●	●	●
		6/4-6/26 74		25.9	RC	●	●	●	●	●	●
				1.2	RC	●	●	●	●	●	●
				11.6	RC	●	●	●	●	●	●
				18.9	RC	●	●	●	●	●	●
				25.9	URC						
CM-12	40°19.0'N 73°47.5'W	4/8-6/6 74	53.34	1.5	RC	●	●	●	●	●	●
				11.9	RC	●	●	●	●	●	●
				32.6	RC	●	●	●	●	●	●
				39.9	RC	●	●	●	●	●	●
				46.9	RC	●	●	●	●	●	●
		6/6-6/26 74		1.5	RC	●	●	●	●	●	●
				11.9	RC	●	●	●	●	●	●
				32.6	RC	●	●	●	●	●	●
				39.9	RC	●	●	●	●	●	●
				46.9	RC	●	●	●	●	●	●

Table 1. Continued.

4. TIDAL CURRENT ANALYSIS

Background

Oceanographic Surveys Branch's data analysis has usually emphasized the accurate description of the tidal portion of the current record because all previous NOS field programs were primarily conducted in estuaries and nearshore regions. User-oriented analysis products, such as tidal current tables and charts, were the primary results. In these regions, the energy contained in the measured current is almost entirely within the tidal spectrum, excluding forcing such as river flow, which in most cases is treated as a constant. Based on the results of harmonic analysis of 15- or 29-day records, predictions are made for the primary station and verified by direct comparison between predicted and observed values. A nonharmonic, rotary reduction technique is used in calculating the constants which can be used to make predictions indirectly at secondary stations.

These standard NOS techniques were applied to the current meter measurements collected in the New York Bight to describe the tidal portion of the current record. Table 1 specifies current meter data for which harmonic analysis and rotary reductions were performed. Definitions of the major harmonic constants, for stations located in the apex region, are given in the appendix. Using the harmonic analysis technique for the calculation of the amplitude and phase of each tidal constituent, the values obtained should be independent of the observational period at a given location; if the results vary, they are unreliable or "unstable." An investigation of the reliability of calculations for north and east components of the harmonic constants was performed. Large variability occurred in the calculation of the harmonic constants, especially for components perpendicular to the shoreline and for both components of the diurnal constituents. This "instability" will be discussed later in this report.

Tidal Current Constituent Ellipses

In unconfined or partially confined regions (such as the New York Bight Apex), the tide-generating forces, acting with the Earth's rotation, result in tidal currents whose direction of flow changes continuously through 360°. Similarly, the flow that can be identified with each harmonic constituent also

Manufacturer: Aanderaa
Parameters Measured: Current Speed, Current Direction, Temperature, Pressure, and Conductivity

Manufacturer Specifications:

Parameter	*Range*	*Accuracy*
Current Speed	*1.5-250 cm/sec*	*±10% of value*
Current Direction	*0-360° magnetic*	*±5° magnetic*
Temperature	*−2.46°C to 21.40°C*	*±0.2°C*
	−0.34°C to 32.17°C	
Pressure	*0-200 PSI*	*±1% of range*
	0-500 PSI	
	0-1000 PSI	
Conductivity	*0-60 mmho*	*±0.05 mmhos*

Recorder: 1/4-inch magnetic tape
Record Format: 10-bit binary words
Sampling rate: 10 minutes
Duration: 60,000 words of information
Processing: Tape to tape transcriber
Mode of operation: Part of an ocean mooring system

Table 2. Current Meter Specifications.

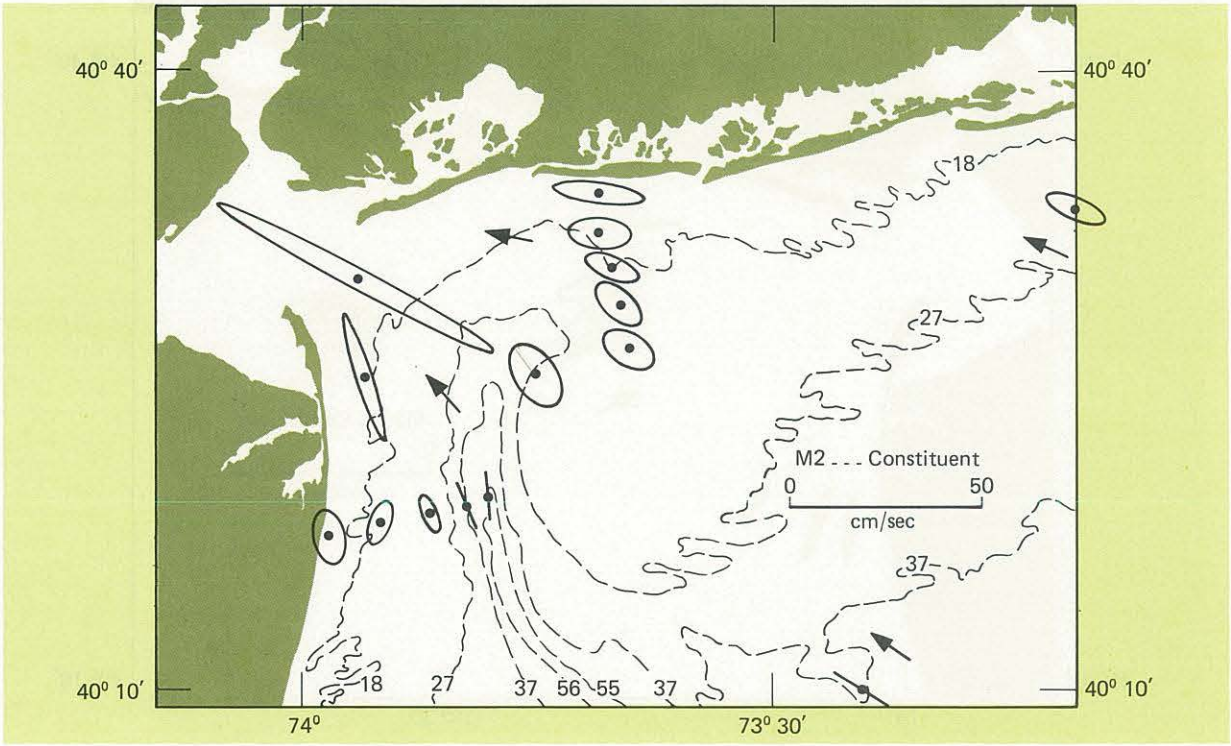

Figure 2. Ellipses for the M2 constituent for bottom observations (<3 m above the bottom) are shown. The centers of ellipses are the station locations. Arrows indicate direction of progress of the M2 progressive wave that occurs when the maximum flood velocity is attained. Current velocities rotate 360° in 12.42 hours. Analysis indicates a counterclockwise rotation for all ellipses, except stations D and G.

exhibits a rotary nature which can be illustrated by means of a harmonic constituent ellipse. Each ellipse (e.g., an M2 ellipse or a K1 ellipse) is determined by the endpoints of a series of vectors describing the flow over one constituent period. These constituent ellipses can be calculated by:

$$V(E) = A(1)\cos(nt) + B(1)\sin(nt)$$
$$V(N) = A(2)\cos(nt) + B(2)\sin(nt)$$

where:

V(E) and V(N) are the east and north velocity components (cm/s), respectively; and

$$A(1) = H(E)\cos(KAPPA(E))$$
$$A(2) = H(N)\cos(KAPPA(N))$$
$$B(1) = H(E)\sin(KAPPA(E))$$
$$B(2) = H(N)\sin(KAPPA(N))$$

where:

H(E), KAPPA(E), and H(N), KAPPA(N) are the amplitude (cm/s) and phase (degrees) of a given harmonic constituent for the east and north components, respectively.

The parameters of the ellipses calculated (by the method described by Doodson and Warburg (1944) and discussed by Swanson (1971)) are:

(1) W(1) and W(2): the magnitude of the major and minor axes in cm/s, respectively. W(1) is the magnitude of the maximum velocity attained.

(2) THETA(1) and THETA(2): the orientation of the major and minor axes, respectively, relative to east in a counterclockwise direction. THETA(1) is the direction of progress of the tidal constituent.

(3) Phase lag: the difference in degrees between the time an astronomical force occurs at the local meridian and the actual current response (e.g., for the M2, the difference between the time the lunar transit passes over the local meridian and the maximum current response).

(4) Rotation: if THETA(2) = THETA(1)−90°, then the rotation is clockwise. If THETA(2) = THETA (1) +90°, then the rotation is counterclockwise.

Table 1 identifies stations for which tidal current ellipse calculations were performed. Figures 2 through 5 represent the analysis of the semidiurnal M2 constituent; figures 6 and 7 represent the diurnal K1 constituent.

For the semidiurnal constituents, M2, N2, and S2, the calculations of THETA(1) (orientation of the ellipse) are consistent. Slight variations occur in calculations of W(1) and the ratio of W(2)/W(1) (relative shape of the ellipse). Calculations for the phase lag, except for bottom observations, are spatially incoherent, but the directions of rotation are relatively consistent. Large deviations in W(1) and W(2)/W(1) occur in the calculations for the K1 and O1 constituents, but THETA(1) and the direction of rotation are consistent.

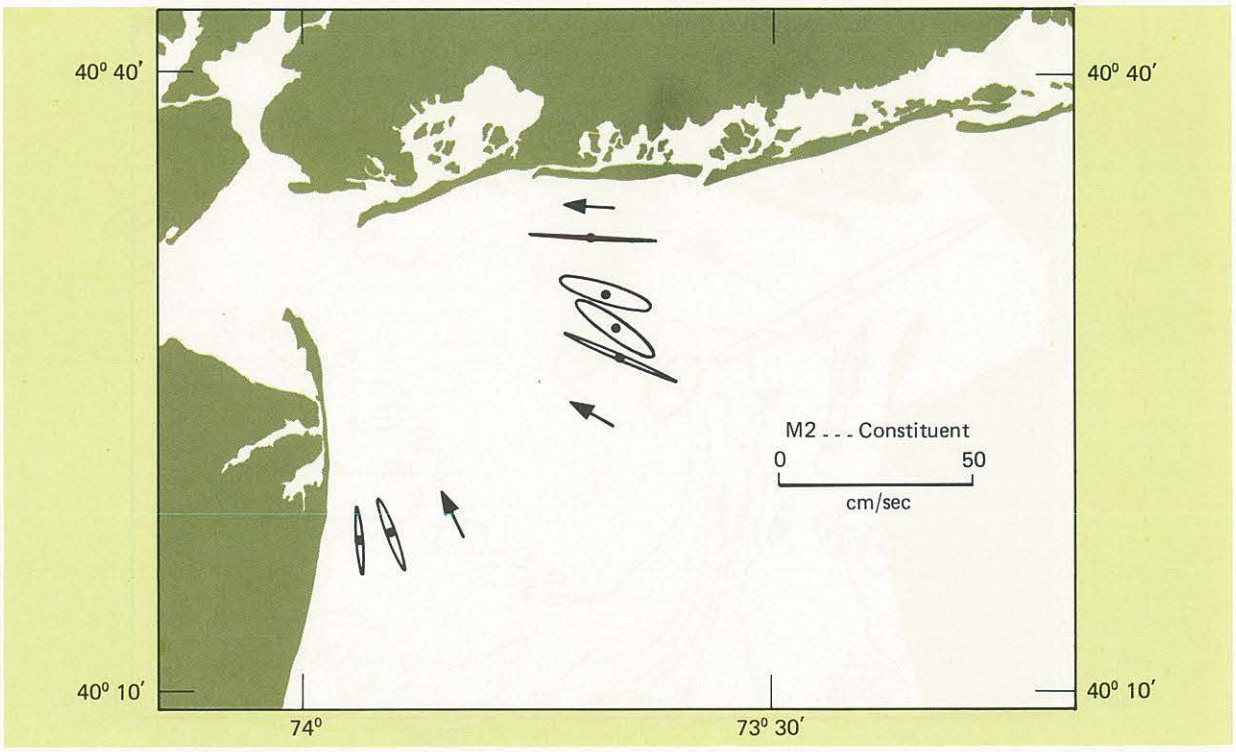

Figure 3. Ellipses for the M2 constituent for observations between 4 and 7 m above the bottom are shown. Arrows indicate direction of progress of the M2 progressive wave that occurs when the maximum flood velocity is attained. Current velocities rotate 360° in 12.42 hours. Analysis indicates a counterclockwise rotation for all ellipses.

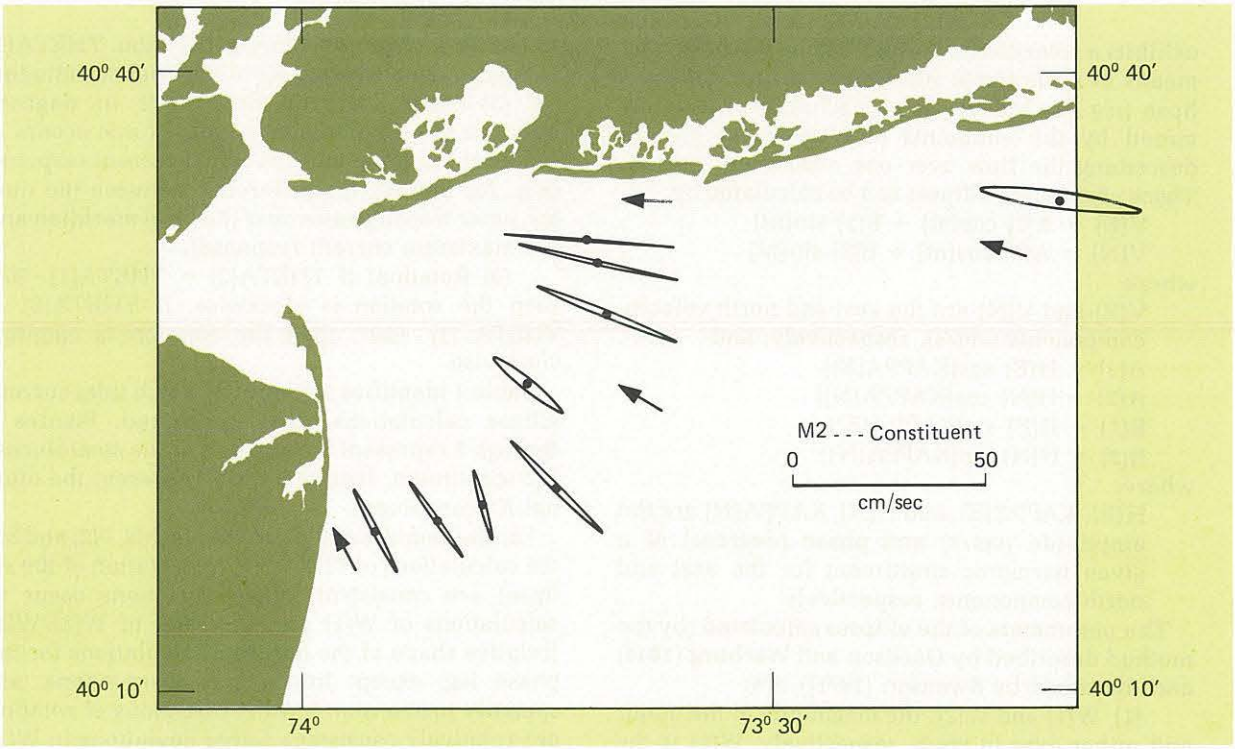

Figure 4. Ellipses for the M2 constituent for observations approximately 8 m above the bottom are shown. Arrows indicate direction of progress of M2 progressive wave that occurs when maximum flood velocity is attained. Current velocities rotate 360° in 12.42 hours. Analysis indicates a clockwise rotation, except stations K and ST-4 rotate counterclockwise.

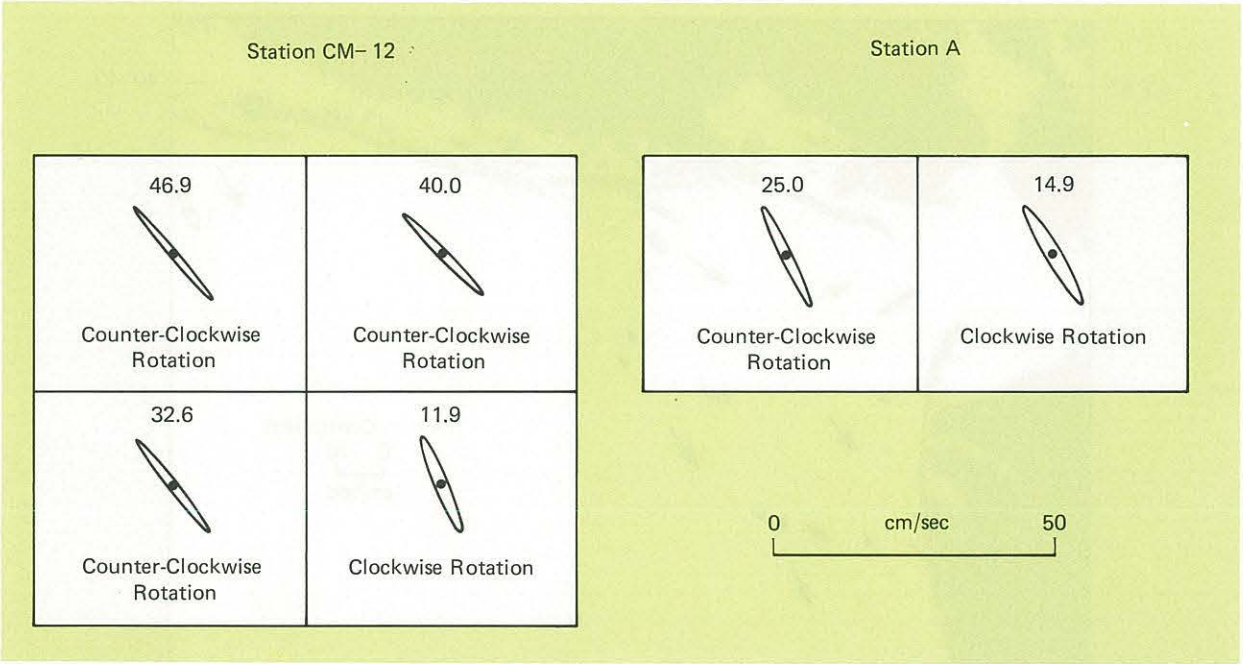

Figure 5. Ellipses for the M2 constituent for near surface observations for stations CM-12 and A are shown. Depths indicated are meters above the bottom.

Magnitude and Orientation of the M2 and K1 Constituent Ellipses

Figures 2 through 4 represent the semidiurnal M2 constituent ellipses for three-depth levels. Direction of progress of the M2 constituent is consistent for all three-depth levels; this direction is west along the New York coast, turning northwest toward the mouth of the Hudson River, and north along the New Jersey coast. Along the New York coast at approximately 8 m above the bottom, velocities of 20 cm/s occur decreasing to 10 cm/s along the New Jersey coast. Figure 5 illustrates the vertical structure of the M2 constituent for stations CM-12 and A. The general vertical structure indicates decreasing velocities with increasing depth from the surface. The magnitude of the semidiurnal constituent is strongest (approximately 40 cm/s) for station D, located at the mouth of the Hudson River, at 1.0 m above the bottom.

Figures 6 and 7 represent the diurnal K1 constituent for two-depth levels. The direction of progress of the diurnal constituent is consistent for most of the observations; this direction is southwest along the New York coast, turning northwest toward the mouth of the Hudson River, and south-southwest along the New Jersey coast. The maximum speed for near-bottom observations is 5 cm/s; for observations between 4 and 8 m above the bottom, maximum speeds of 8 cm/s occur. At a given station location over different observational periods, large variations in the calculations of W(1), W(2)/W(1), and phase lag occur especially during the spring season when extremely large values are present. These large inconsistencies again indicate the "instability" of the harmonic analysis technique used in calculation of the diurnal harmonic constants for this region. Preliminary results indicate the insufficiency of performing a harmonic analysis based on 15-day records.

The influence of the temporal variation of the land-sea breeze on the calculation of the harmonic constants for the diurnal constituents must be investigated. Schureman (1958) stated that land-sea breeze will occur at the same frequency as S1, and the synodic period for S1/K1 is 365.243 days; therefore, it will take a yearlong data series to separate K1 from the land-sea breeze. Haight (1936) stated that at St. Johns Lightship, the effect of the rotary land-sea breeze increased the S1 constituent from 1 or 2 percent of M2 to 52 percent of M2. The effect of other nontidal frequencies on the calculations of the harmonic constants, which are often predominant in this region, must also be studied. Other techniques used for calculating the harmonic constants, such as least-squared techniques and the response method, must also be investigated as to "instability" problems.

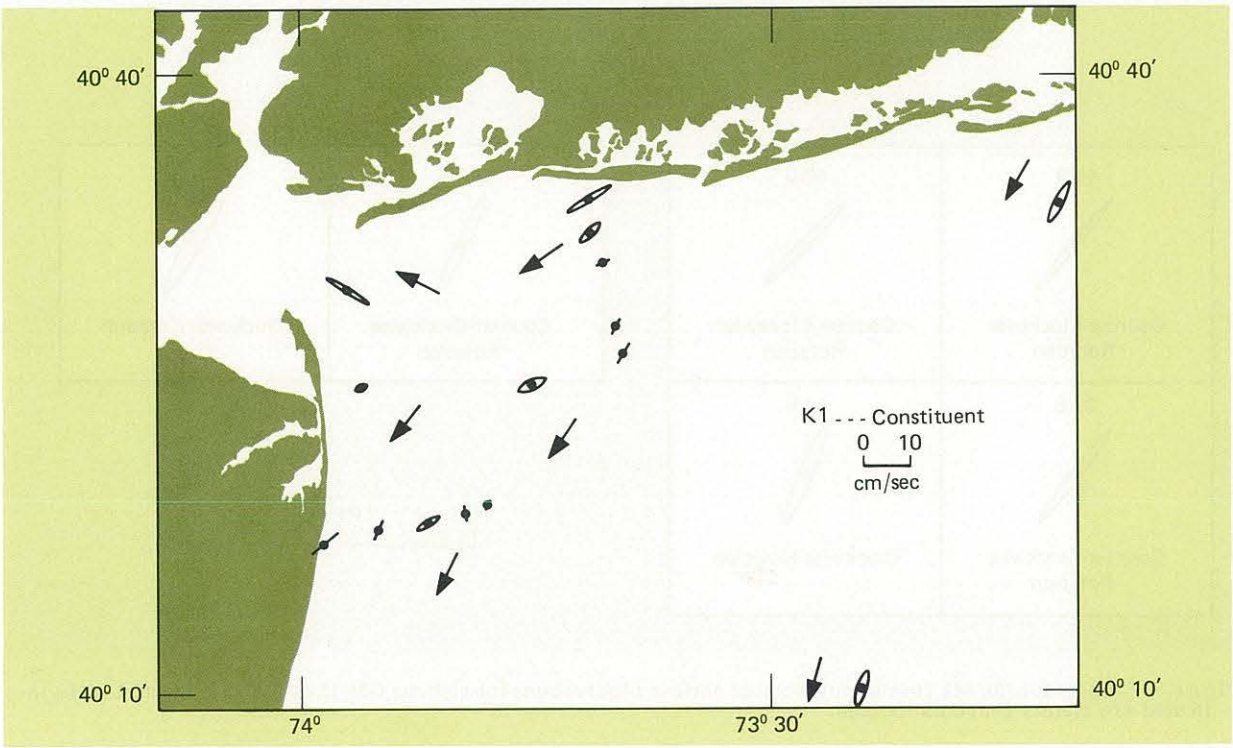

Figure 6. Ellipses for the K1 constituent for bottom observations (<3 m above the bottom) are shown. Center of ellipse is station location; arrows indicate direction of progress of the K1 progressive wave that occurs when the maximum flood velocity is attained. Current velocities rotate 360° in 23.93 hours. Analysis indicates a clockwise rotation for stations: CM-1, CM-2, CM-7, K, CM-10, ST-4, and G; and counterclockwise rotation for stations: D, R, CM-3, CM-5, CM-6, CM-11, A, and H.

Rotation of Tidal Current Constituent Ellipses

The direction of rotation of the tidal current ellipse can be the result of: (1) direct response to tide-generating astronomical forces; (2) effect of Earth's rotation; (3) effect of shelving coasts; and (4) friction. For semidiurnal constituents, the result of both the direct response to tide-generating astronomical forces and the rotation of a "frictionless" Earth is a clockwise rotation in the Northern Hemisphere. Calculations of rotation for the M2 constituent indicate a clockwise rotation for observations between 15 and 8 m above the bottom. Defant (1961) stated that the influence of friction (which results in a formation of a bottom boundary layer) on a constituent ellipse is a decrease in W(1), an increase of W(2)/W(1), a retardation of phase, and a reversal of rotation.

The existence of a boundary layer up to 7 m above the bottom can be inferred by the changing shape and reversal of rotation from clockwise to counterclockwise of the M2 constituent ellipse. The reversal of rotation of the M2 ellipse for stations along the coast exhibits the influence of shelving coasts. Reversal of rotation, shown in figure 5, may be the manifestation of a surface boundary layer.

For diurnal constituents, the direct response to the tide-generating forces is a counterclockwise rotation between 0° and 45°N. However, the effect of rotation of a "frictionless" Earth is a clockwise rotation in the Northern Hemisphere. Calculations indicate 74 percent of all observations rotate clockwise. For near bottom observations, 61 percent rotate clockwise; and for the remaining observations, 83 percent rotate clockwise. These calculations indicate the primary forcing mechanisms are the Earth's rotation and bottom friction.

Phase information for the semidiurnal M2 and the diurnal K1 constituents at selected levels is illustrated by cophase lines and current directions at a specific stage of a tidal current constituent in figure 8 and in figures 9 through 12, respectively. Time is referenced to the time of maximum astronomic force for a given constituent over the local meridian. Phase information appeared spatially incoherent for other depth levels.

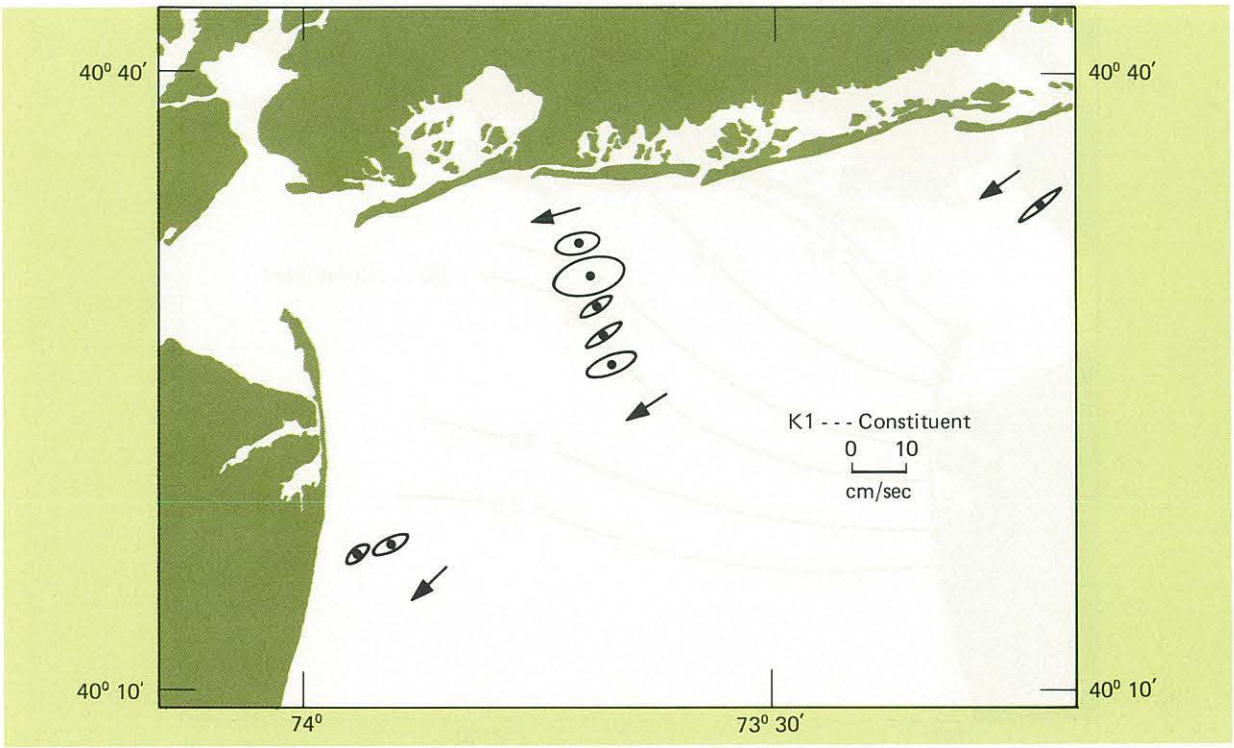

Figure 7. Ellipses for the K1 constituent for observations between 4 and 8 m above the bottom are shown. Center of ellipse is station location; arrows indicate direction of progress of the K1 progressive wave that occurs when the maximum flood velocity is attained. Current velocities rotate 360° in 23.93 hours. Observations for stations CM-2 through CM-6 were collected from May 22 through June 22, 1974, and for stations CM-8 and CM-9 were collected from April 24 through May 28, 1974. Analysis indicates a clockwise rotation for all stations, except station 6.

5. LOW FREQUENCY ANALYSIS

Background

In describing the circulation of the apex region, a comparison between the energy contained in the tidal frequency band and the energy contained in the nontidal frequency bands must be made to determine the significance of the tidal regime. The tidal current is defined as a periodic current originating from astronomical forces; the net flow over each period is zero. A "residual" constant is calculated over the entire observational period which contains the effect of meteorological conditions and river inputs during the observational period; this constant does not give insight into the temporal variability of the nontidal regime.

In other major areas investigated by NOS, the energy in the nontidal bands has been small (excluding river inputs). However, in the New York Bight Apex, a high percentage of the total energy is present in the nontidal low-frequency band, and thus temporal variations of the "residual" are important. To interpret this nontrivial low-frequency energy, standard analysis procedures were expanded to include the following:

(1) Using the original 10-min edited current meter records, the following were determined: the magnitude and direction of mean current and a direction histogram over the maximum number of complete tidal cycles for the observational period; and the energy level and power spectra for the north and east components.

(2) Original data were then smoothed to hourly values and filtered using a Doodson filter, a 39-hr low-pass filter which removes 99.79 percent of all diurnal frequencies and 99.48 percent of all semidiurnal frequencies (Groves, 1955). For both the low frequency or "doodsoned" (residual) and the high frequency (mainly tidal) series, direction histograms were plotted, and the percentages of total energy contained in each series and power spectra for the north and east components were computed.

Table 1 identifies stations for which this time series analysis has been performed. Calculations of energy contained in the high and low frequency bands varied from over 90 percent occurring in the high frequency band for stations D and I to 80 percent occurring in the low frequency band at station A. In general, however, calculations revealed an approximate equal partitioning at the 39-hr period.

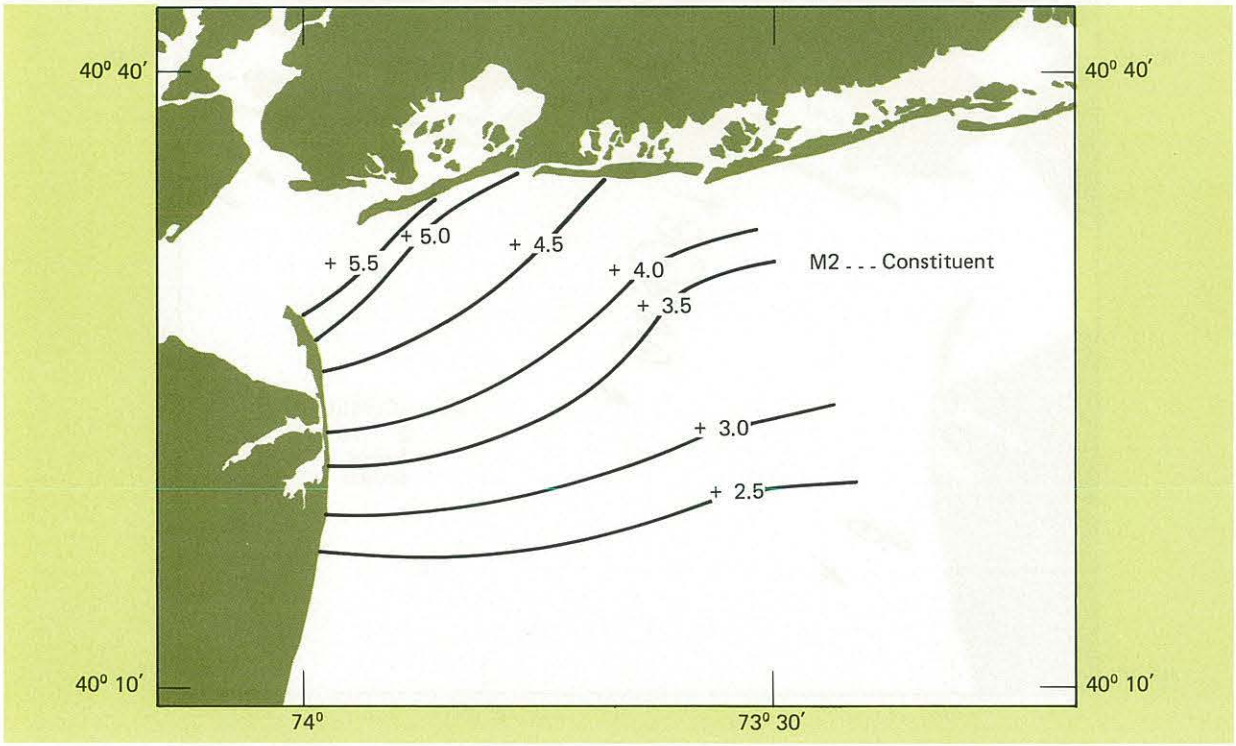

Figure 8. Cophase lines for the semidiurnal M2 constituent for bottom observations. Contours represent time of maximum M2 flood (in hours referred to the lunar transit over the local meridian).

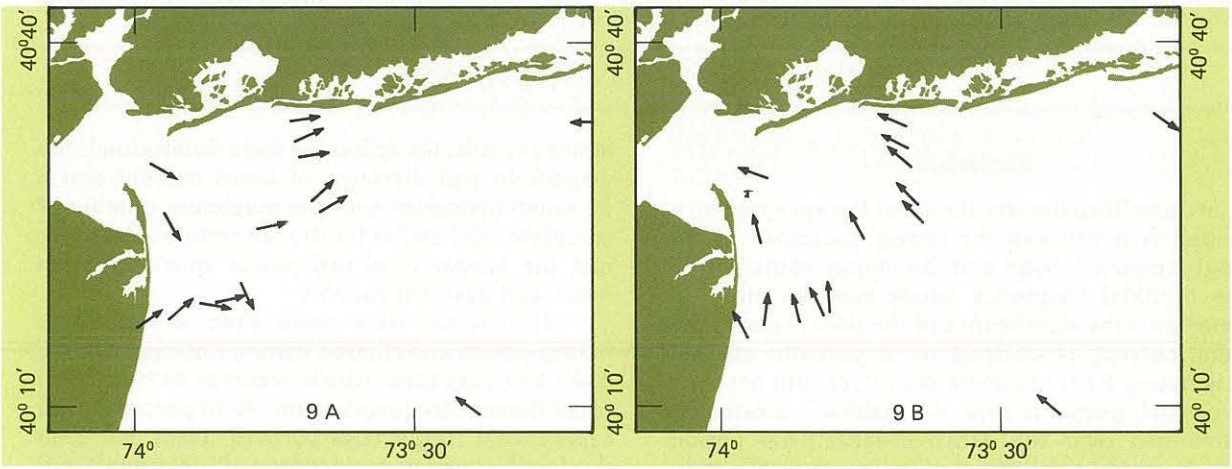

Figure 9. Arrows represent direction of the semidiurnal M2 constituent for the bottom observations. Figure 9A represents directions at the time of lunar transit over the local meridian. Figure 9B represents directions 3 hours and 6 minutes after the lunar transit passes through the local meridian.

Calculations appeared invariant with depth at a given station.

Wind and Density Effects

Mean values of the currents for the 1973 observations indicate a clockwise circulation which is stronger in the winter season. These results are consistent with the circulation reported by Charnell and Mayer (1975). Figures 13 through 15 illustrate the mean circulation derived from current meter information collected during the spring of 1974; mean wind at Kennedy Airport at the same time periods is also illustrated.

The circulation in the New York Bight Apex for the spring of 1974 can be determined using the current meter observations, wind observations collected at Kennedy Airport, and the physical oceanographic data presented in *NOAA Data Report MESA-1* (Hazelworth, 1975). During the period from April 9 to 24, 1974, stratification had

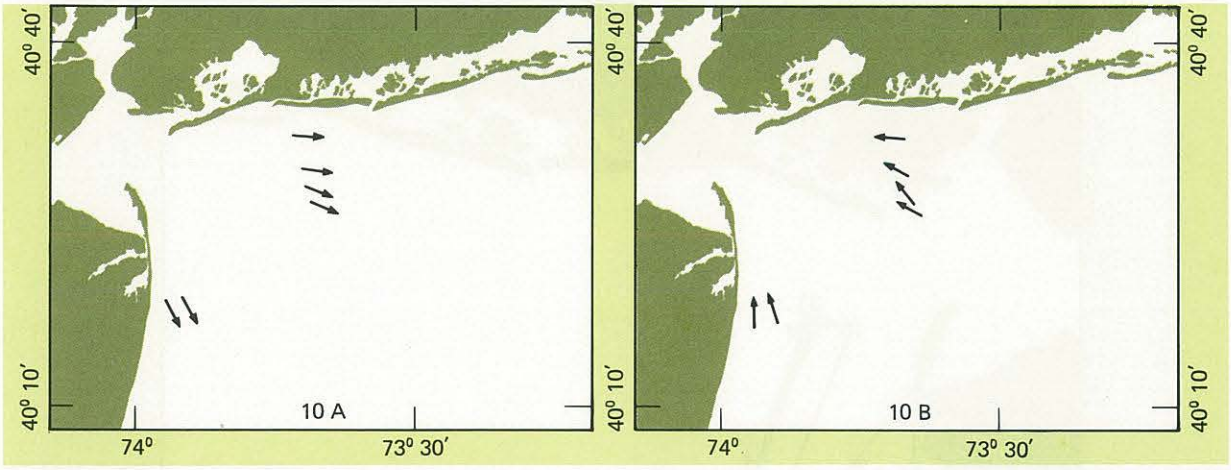

Figure 10. Arrows represent direction of the semidiurnal M2 constituent for observations between 4 and 7 m above the bottom. Figure 10A represents directions at the time of the lunar transit over the local meridian. Figure 10B represents directions 3 hours and 6 minutes after the lunar transit passes through the local meridian.

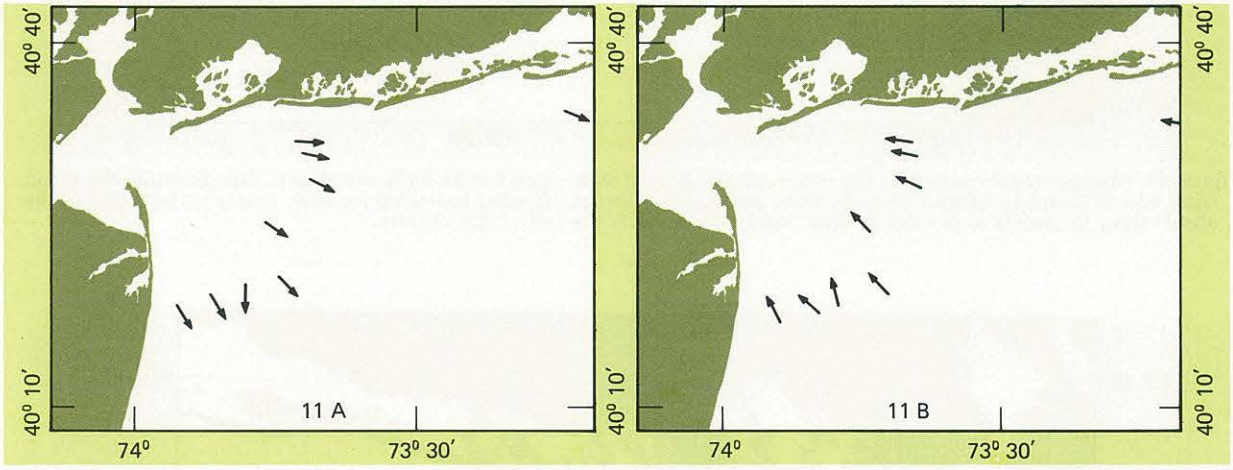

Figure 11. Arrows represent direction of the semidiurnal M2 constituent for observations 8 m above the bottom. Figure 11A represents directions at the time of the lunar transit over the local meridian. Figure 11B represents directions 3 hours and 6 minutes after the lunar transit passes through the local meridian.

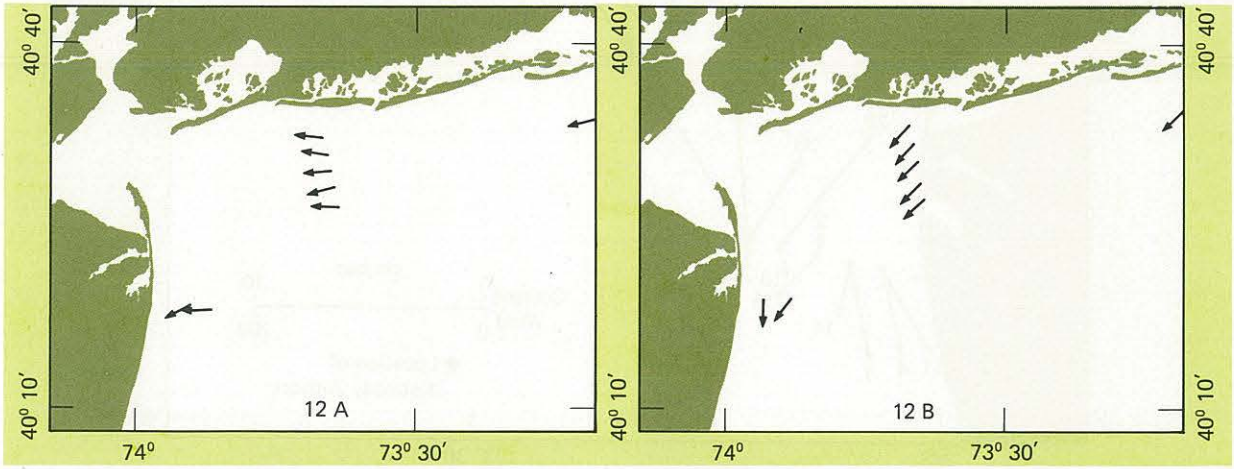

Figure 12. Arrows represent direction of the diurnal K1 constituent for observations between 4 and 8 m above the bottom. Observations for CM-2 through CM-6 were collected from May 22 through June 22, 1974, and for CM-8 and CM-9 from April 24 through May 28, 1974. Figure 12A represents directions at the time of maximum equilibrium force for the K1 constituent over the local meridian. Figure 12B represents directions 6 hours after the maximum equilibrium force for the K1 constituent passes through the local meridian.

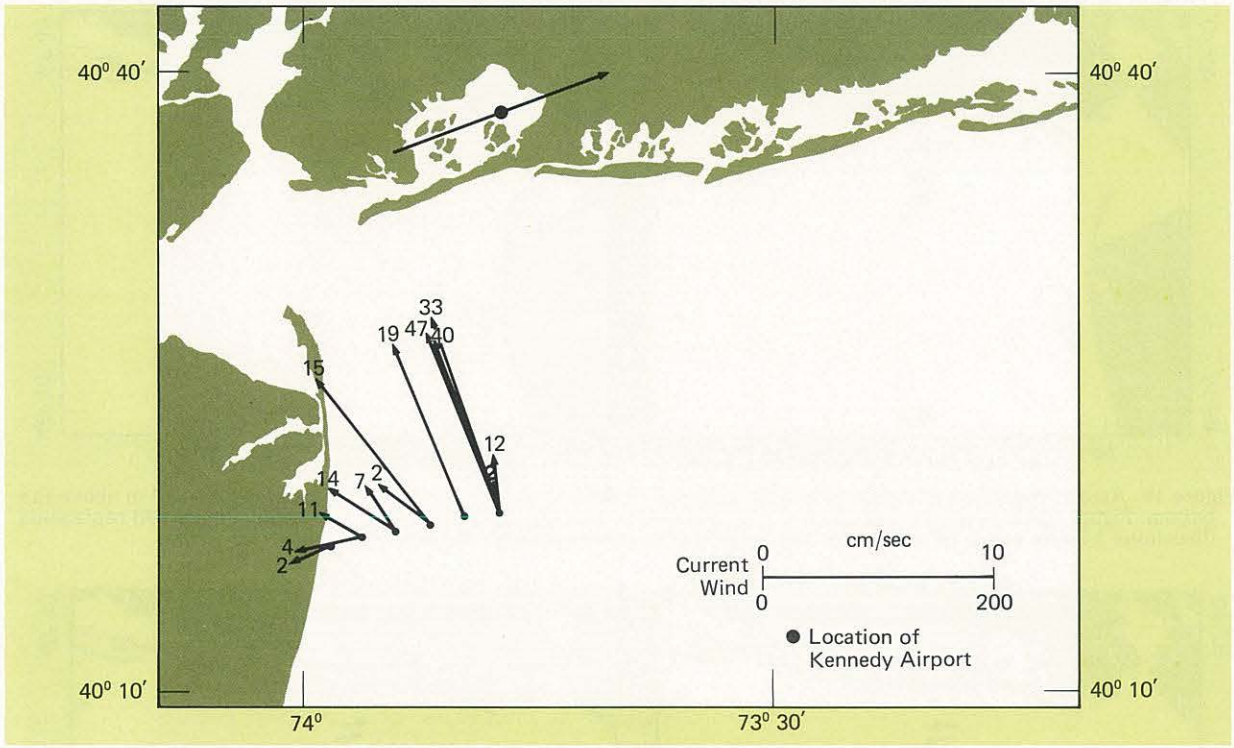

Figure 13. Mean current vectors for the observational period from April 9 to 24, 1974, are shown. The direction the mean wind sets at Kennedy Airport over the same period is indicated. Number indicated for each vector is the depth of the observation in meters above the bottom; station location is the tail of the vectors.

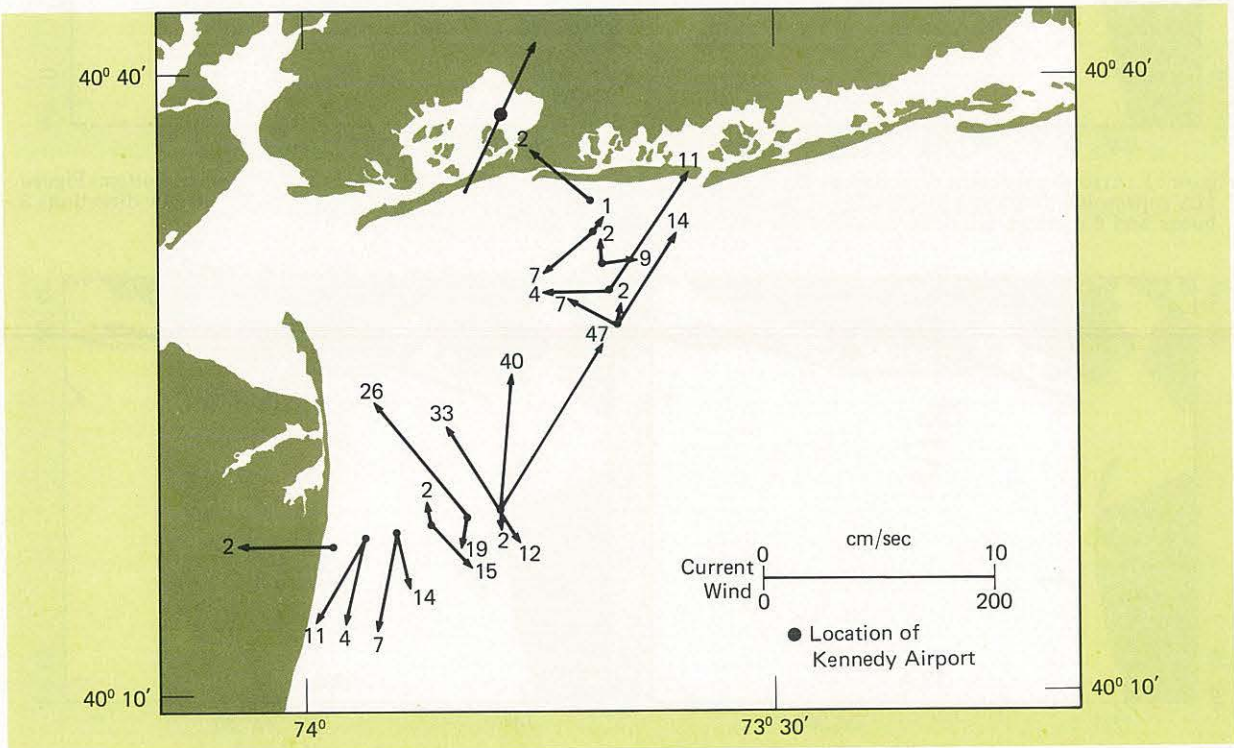

Figure 14. Mean current vectors for the observational period from April 26 to May 27, 1974, are shown. The direction the mean wind sets at Kennedy Airport over the same period is indicated. Number indicated for each vector is the depth of the observation in meters above the bottom; station location is the tail of the vectors.

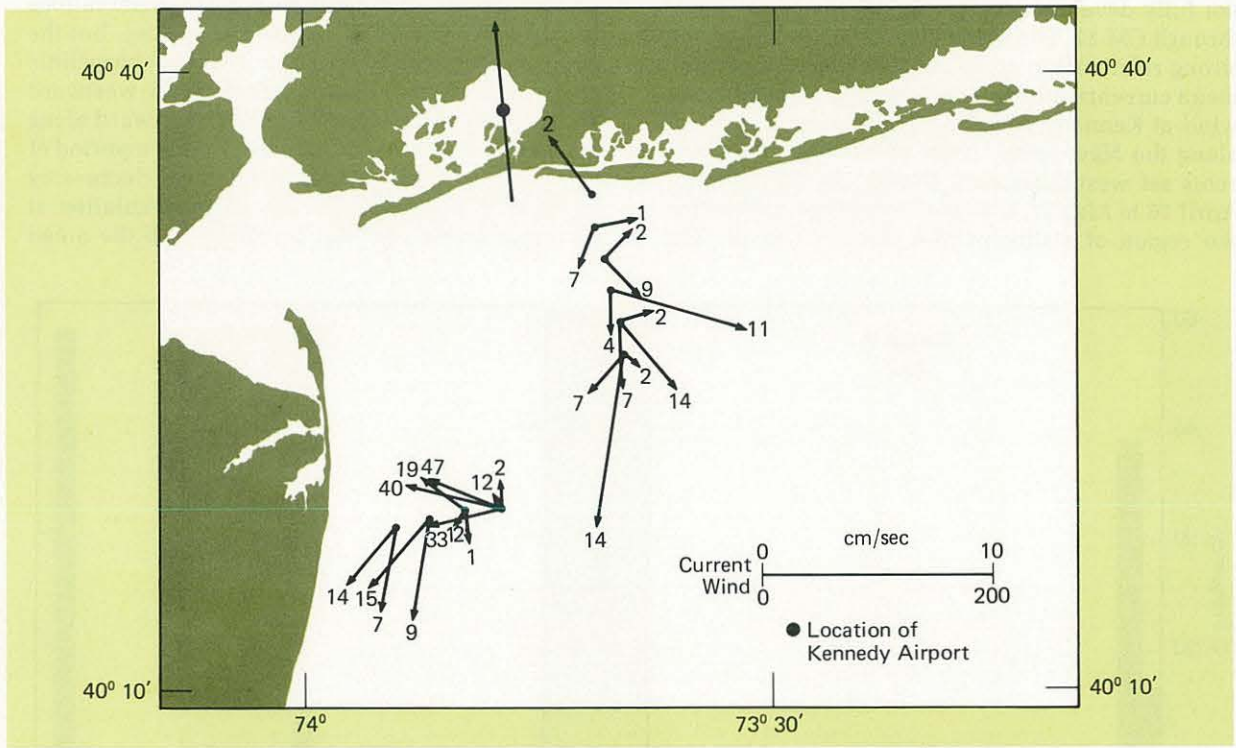

Figure 15. Mean current vectors for the observation period from June 7 to 24, 1974, are shown. The direction the mean wind sets at Kennedy Airport over the same period is indicated. Number indicated for each vector is the depth of the observation in meters above the bottom; station location is the tail of the vectors.

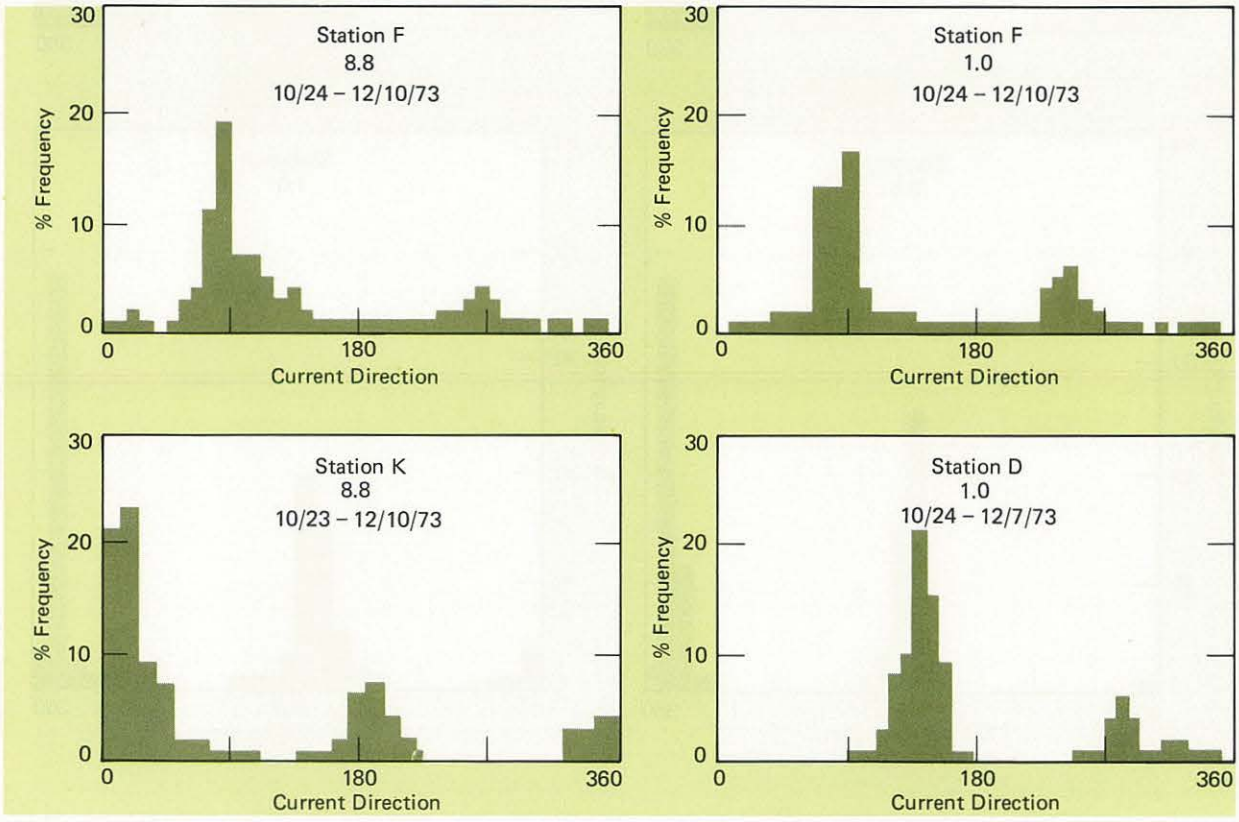

Figure 16a. Direction histograms (°T) of the "doodsoned" current meter observations for stations F, K, and D are shown. Observational periods for the calculations are shown. Depths indicated are meters above the bottom.

not fully developed in the region of stations CM-7 through CM-12. The mean circulation indicates the strong relationship at all depth levels between the mean currents and the east component of the mean wind at Kennedy Airport, except near the bottom along the New Jersey coast where the mean currents set west-southwest. During the period from April 26 to May 27, a deep thermocline existed for the region of stations CM-4 through CM-12. The mean current values of near surface observations have a tendency to follow the mean wind, but the near bottom values indicate a strong baroclinic mode. The near bottom current flows westward along the New York coast, turning southward along the New Jersey coast. From June 7 to 24, a period of increasing density stratification and decreasing depth of the thermocline, the mean circulation at all depth levels does not correlate with the mean

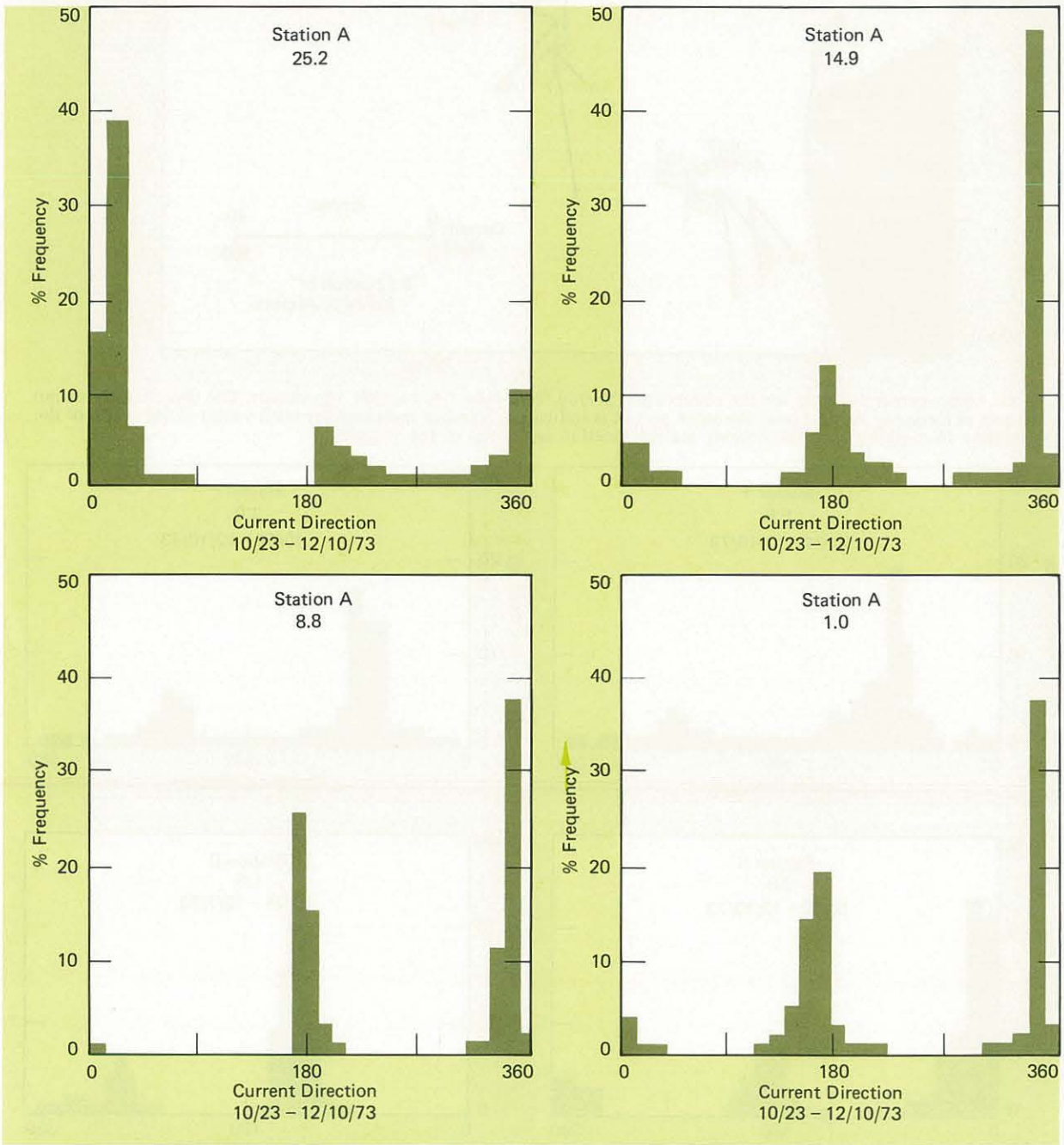

Figure 16b. Direction histograms (°T) of the "doodsoned" current meter observations for station A are shown. Observational periods for the calculations are shown. Depths indicated are meters above the bottom.

wind, but has a southward tendency throughout the New York Bight Apex.

Mean circulation does not allow insight into the temporal variations of flow. A statistical interpretation of the circulation may be attained by calculating the percentage occurrence of a direction from a given series of directions. Figure 16 represents direction histograms of "doodsoned" current meter observations for stations A, F, K, D, and CM-12 for the observational periods indicated. Direction histograms for stations A and CM-12 illustrate statistical vertical variations of the "doodsoned" current observations. All histograms exhibit a two-directional modal characteristic, except for the near surface measurements at station CM-12. Statistical circulation patterns can be inferred using mean values and direction histograms, but are limited to the observational period. A statistical

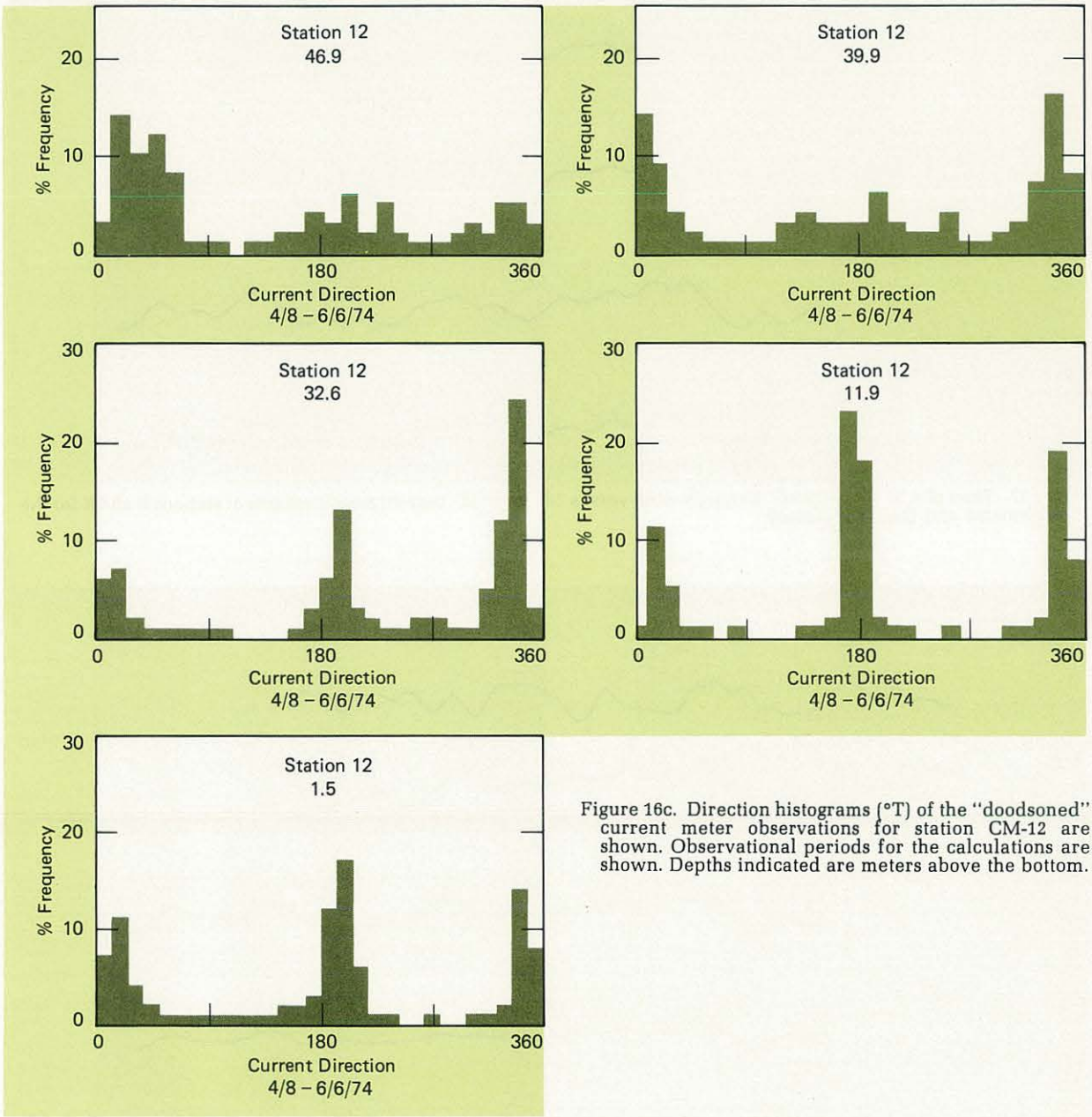

Figure 16c. Direction histograms (°T) of the "doodsoned" current meter observations for station CM-12 are shown. Observational periods for the calculations are shown. Depths indicated are meters above the bottom.

Figure 17 through 24. Time plots of "doodsoned" (39-hr low-pass filtered) Kennedy Airport wind data versus "doodsoned" current measurements for 1973 and 1974 observations. Station name and depth of current meter observations (in meters above the bottom) are indicated; speeds are in cm/s.

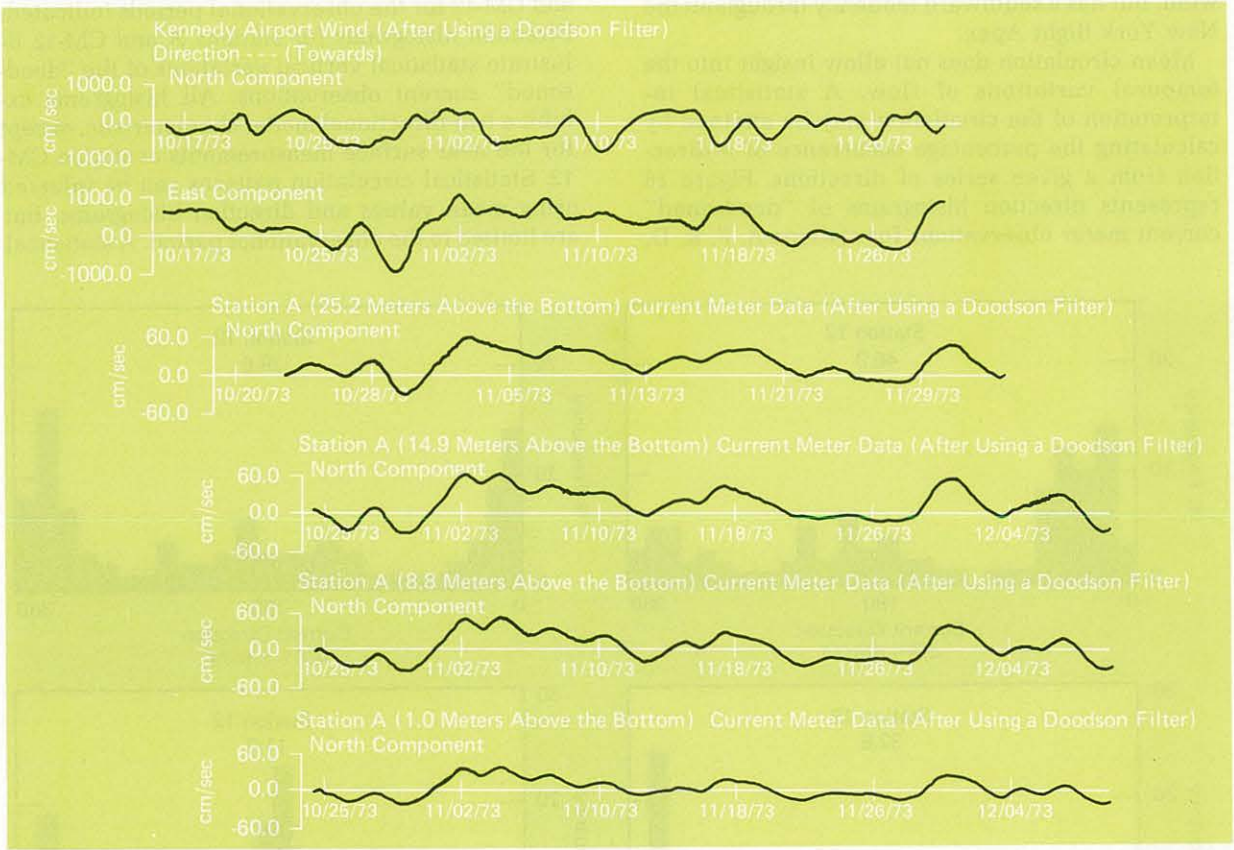

Figure 17. Time plot of "doodsoned" Kennedy wind versus "doodsoned" current measurements at stations F and K for the components and depths indicated.

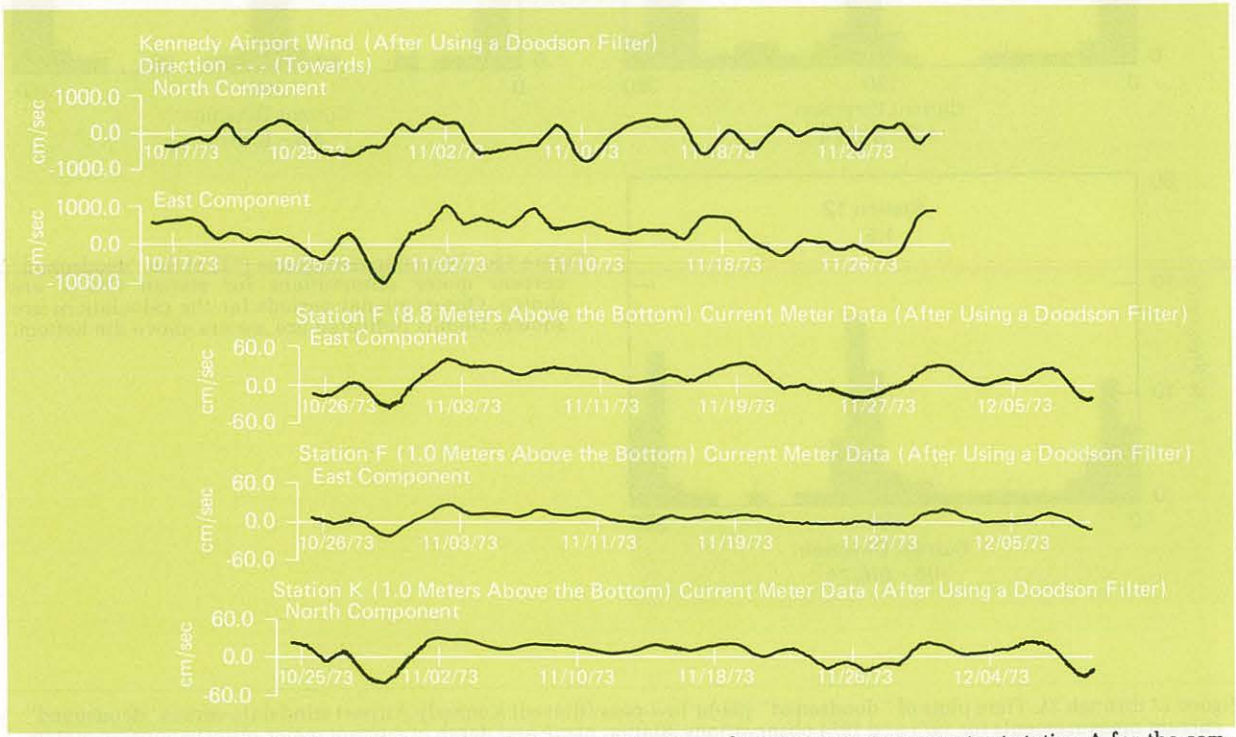

Figure 18. Time plot of "doodsoned" Kennedy wind versus "doodsoned" current measurements at station A for the components and depth indicated.

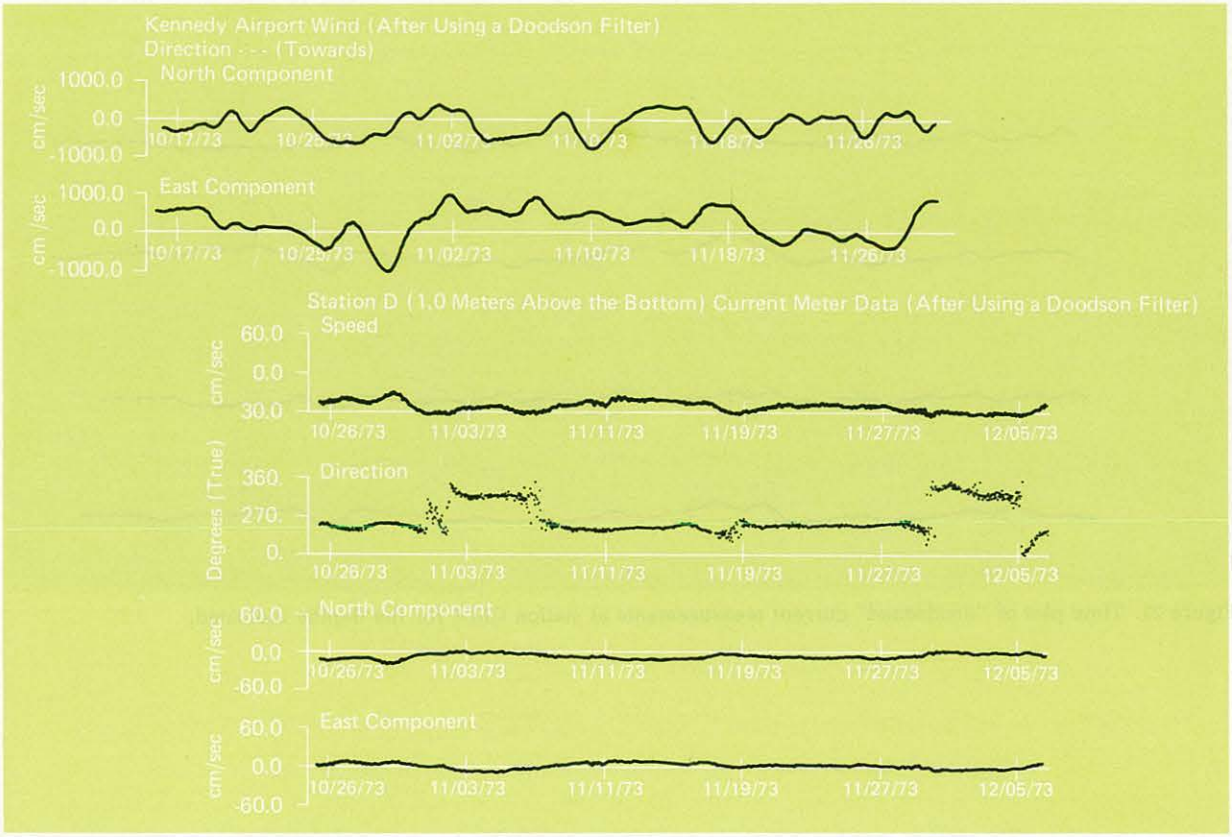

Figure 19. Time plot of "doodsoned" Kennedy wind versus "doodsoned" current measurements at the near bottom meter for station D.

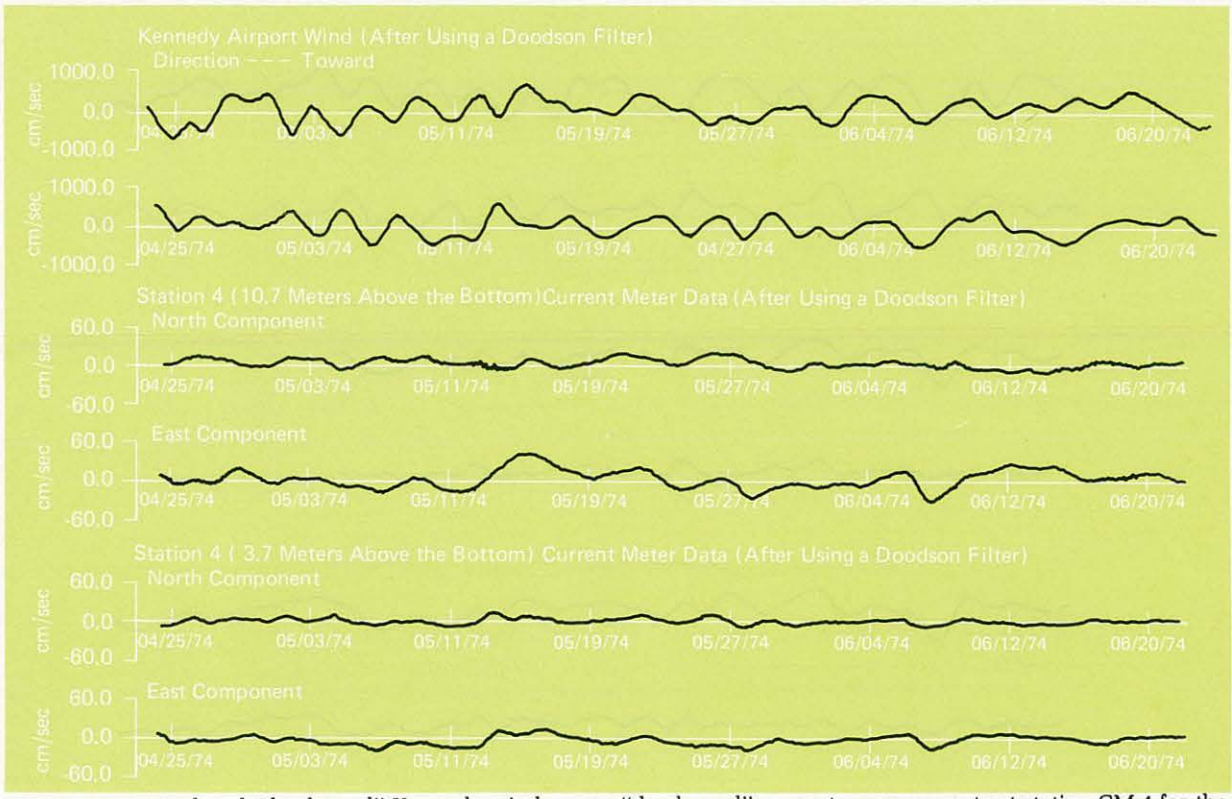

Figure 20. Time plot of "doodsoned" Kennedy wind versus "doodsoned" current measurements at station CM-4 for the depths indicated.

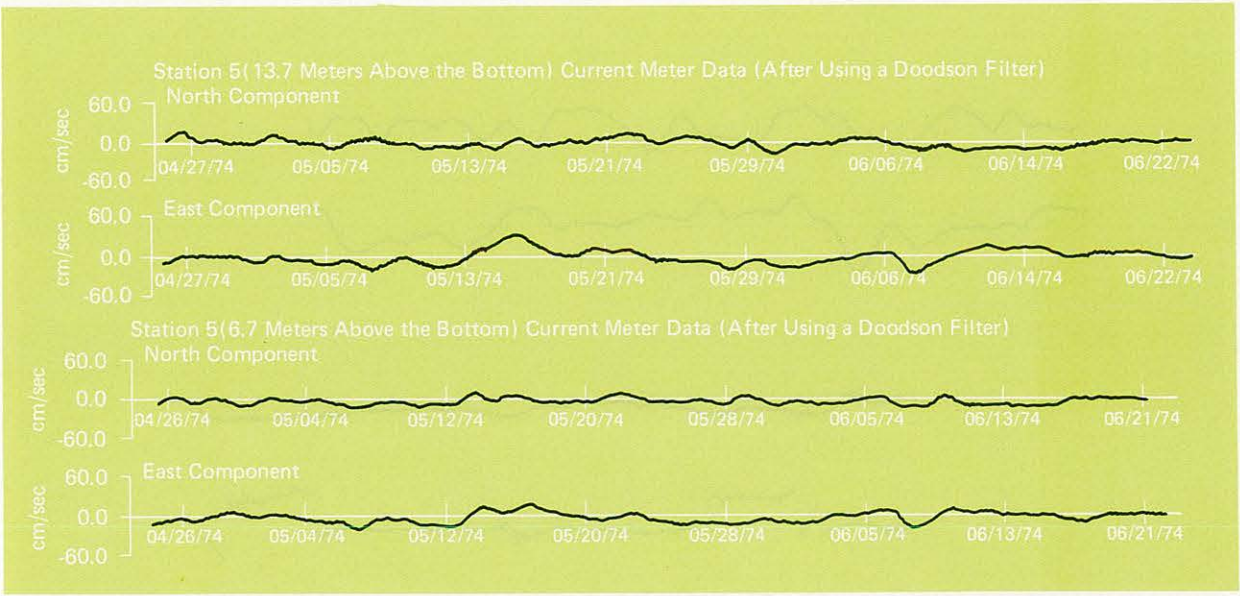

Figure 21. Time plot of "doodsoned" current measurements at station CM-5 for the depths indicated.

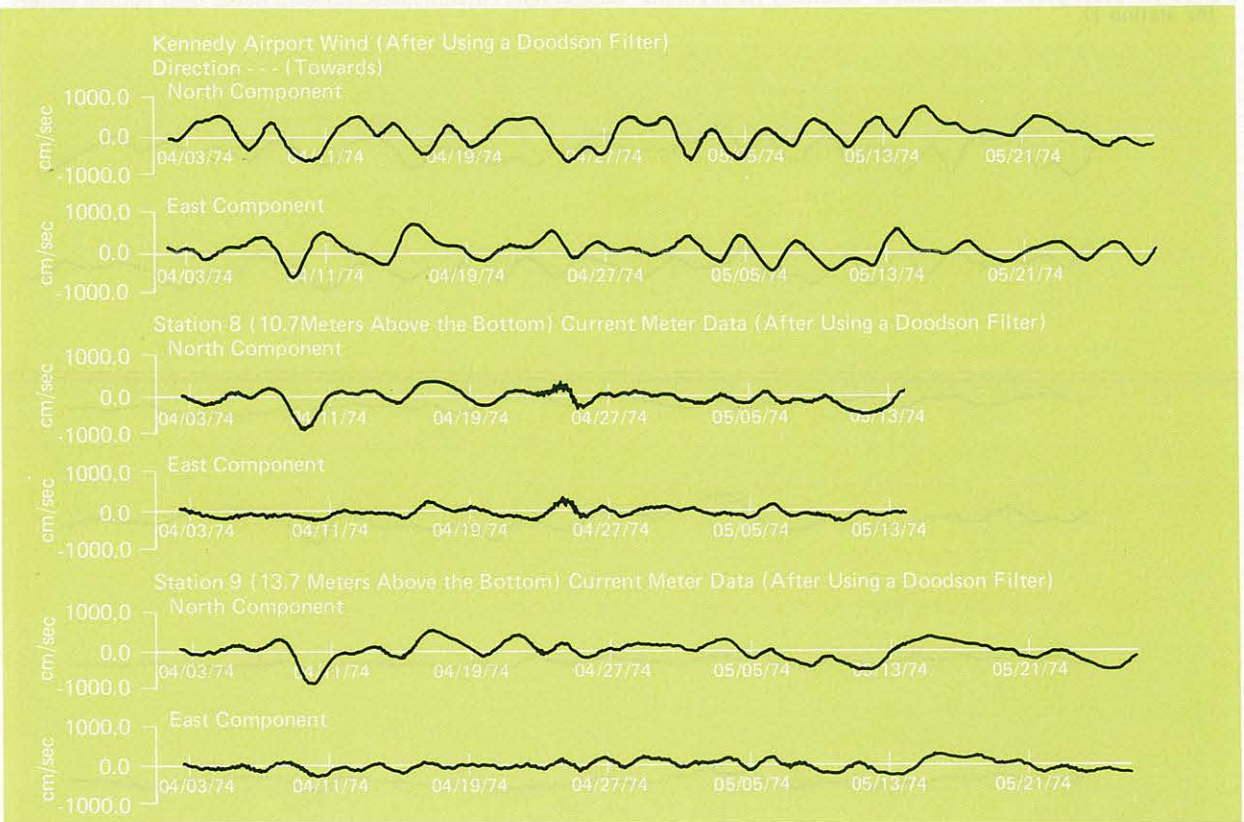

Figure 22. Time plot of "doodsoned" Kennedy wind versus "doodsoned" current measurements at stations CM-8 and CM-9 for the depths indicated.

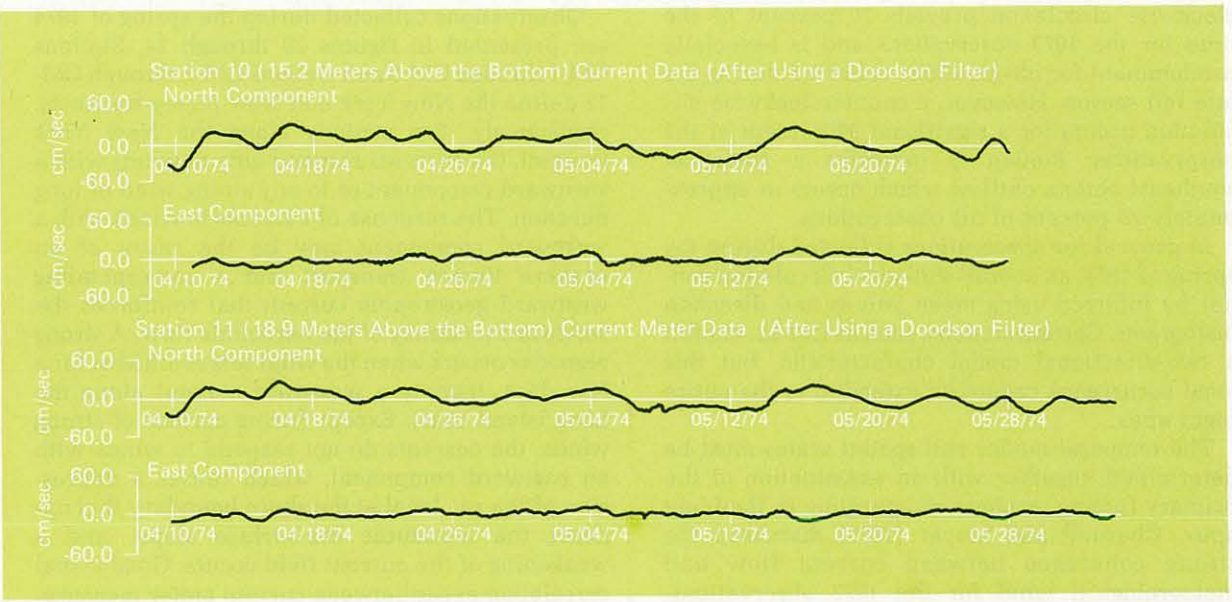

Figure 23. Time plot of "doodsoned" current measurements at stations CM-10 and CM-11 for the depths indicated.

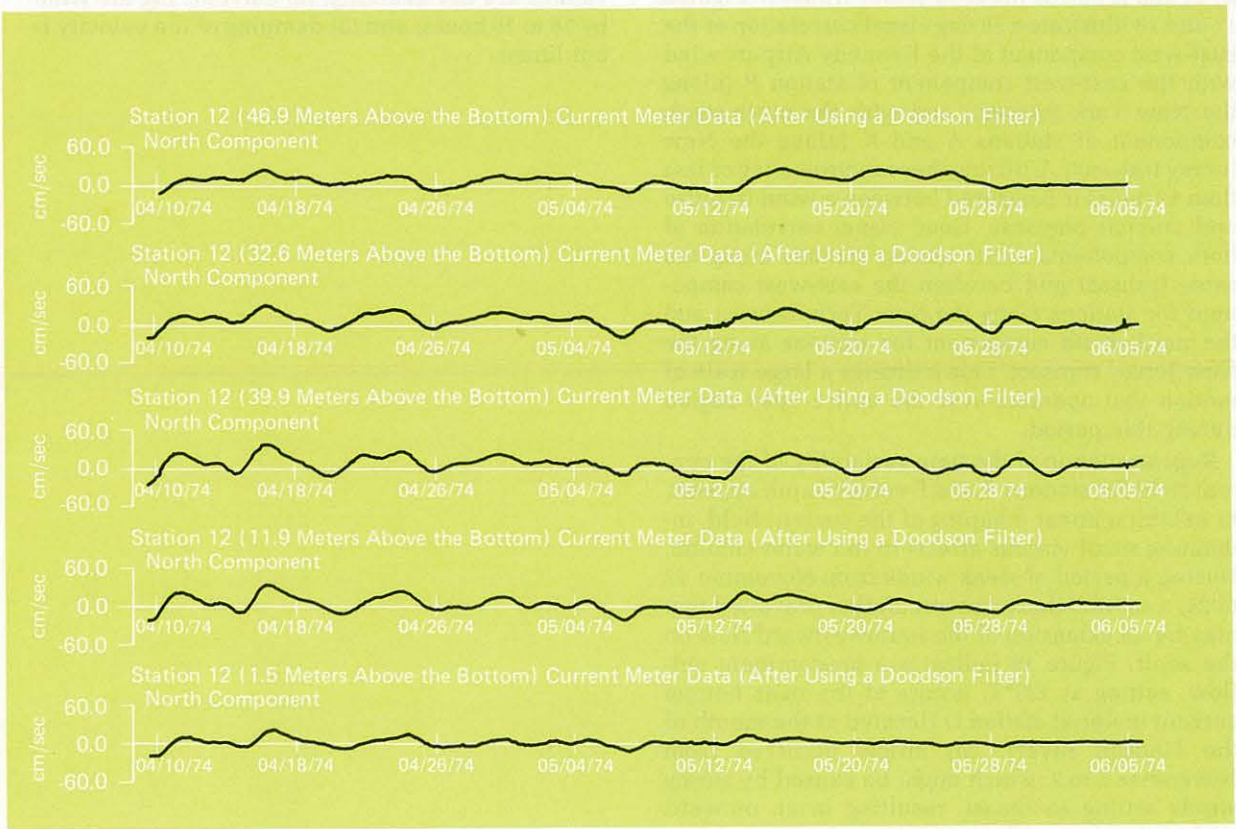

Figure 24. Time plot of "doodsoned" current measurements at station CM-12 from near surface to near bottom depths.

clockwise circulation prevails 70 percent of the time for the 1973 observations and is especially predominant for observations collected during the late fall season. However, a counterclockwise circulation occurs for a significant 30 percent of the observations. Station D indicates a statistical southeast bottom outflow which occurs in approximately 70 percent of all observations.

In general for observations collected during the spring of 1974, an overall statistical circulation cannot be inferred using mean values and direction histograms. Certain stations, such as CM-12, exhibit a two-directional modal characteristic, but this local occurrence cannot be extended to the entire bight apex.

The temporal modes and spatial scales must be determined, together with an examination of the primary forcing mechanism operating in the bight apex. Charnell and Mayer (1975) discussed the strong coherence between current flow and meteorological wind for the 1973 observations. Figures 17 through 24 illustrate the time and spatial relations between "doodsoned" (low-frequency) current meter observations collected at various stations and "doodsoned" (low-frequency) wind observations collected at Kennedy Airport.

Observations collected during the late fall of 1973 are shown in figures 17 through 19. Stations E and F define the New York transect and stations A, B, C, and K define the New Jersey transect. Figures 17 and 18 illustrate a strong visual correlation of the east-west component of the Kennedy Airport wind with the east-west component of station F (along the New York transect) and with the north-south component of stations A and K (along the New Jersey transect). Utilizing these figures, a lag of less than 12 hours is measured between a wind impulse and current response. Good visual correlation of both components exists among stations along the same transect and between the east-west component for stations along the New York transect and the north-south component for stations along the New Jersey transect. This indicates a large scale of motion that operates over the entire apex region during this period.

Representation of the time variability of the current field for stations A and F versus depth appears to exhibit a linear damping of the current field, indicating small viscous effects in the water column. During a period of weak winds from November 22 to 24, a counterclockwise circulation prevailed that may be an extension of the southwestward flow on the shelf. Figure 19 indicates a predominant outflow, setting at 135°T, occurs at the near bottom current meter at station D (located at the mouth of the Hudson River). An inflow occurred from November 1 to 7, which might be caused by strong winds setting southeast, resulting in an outward surface current with a compensatory inward bottom current.

Observations collected during the spring of 1974 are presented in figures 20 through 24. Stations CM-1 through CM-6 and stations CM-7 through CM-12 define the New York and New Jersey transects, respectively. For stations along the New York transect, the currents respond only to winds with a westward component or to any strong wind of long duration. The response of currents to winds with a westward component may be the result of an onshore Ekman transport and a corresponding westward geostrophic current that reinforces the westward tendency of the baroclinic flow. A strong response occurs when the wind sets southwest for a few days, namely a westward current along the Long Island coast. Except during periods of strong winds, the currents do not respond to winds with an eastward component, which causes a depression of the sea level at the shore boundary that opposes the baroclinic sea-surface slope, and a weakening of the current field occurs. Good visual correlation exists between current meter measurements at different station locations and between current measurements at different depths at a given station.

For stations along the New Jersey transect, the relations between 1974 current meter observations and Kennedy wind observations exhibit the same general characteristics as those collected during 1973, except: (1) visual correlations between observations are not as strong; (2) currents lag the wind by 16 to 18 hours; and (3) damping of the velocity is not linear. □

6. SUMMARY

a. The tidal constituents of primary importance in the New York Bight Apex are the M2 and K1 constituents. Calculations of the ellipse parameters for the semidiurnal constituents are relatively consistent throughout the observational period. The direction of progress for the M2 constituent is west along the New York coast, turning northwest toward the mouth of the Hudson River, and north along the New Jersey coast. Large inconsistencies occurred in the calculation of the ellipse parameters for the diurnal constituents, especially the phase lag. Direction of the progress for the K1 constituent was relatively consistent; this direction is southwest along the New York coast, turning northwest toward the mouth of the Hudson River, and south-southwest along the New Jersey coast.

b. There exists a frictional bottom boundary layer extending approximately 7 m above the bottom.

c. In general, the data indicate an approximate equal partitioning of the energy level at the 39-hr period.

d. For the fall season, a statistical clockwise circulation prevails, but a significant percentage of the observations (30%) indicates a counterclockwise circulation. A statistical outflow at station D occurs during 70 percent of the observations, but 30 percent of the observations indicates an inflow toward the Hudson River. The latter seems to be the response to winds setting southeast, resulting in an outward surface current with a compensatory inward bottom flow.

e. For the spring season, the development of stratification and the depth of the thermocline appear to determine the mean circulation. The response of the mean current to the wind is strong in the entire water column when the stratification is weak, but is only in the surface layer when the thermocline is deep in the water column.

f. Temporal variations for stations along the New Jersey transect exhibit a high degree of correlation between the east-west component of Kennedy wind and the north-south component of current meter observations, especially during the fall season. Stations along the New York transect exhibit a high degree of correlation between the east-west component of the Kennedy wind and the east-west component of current observations during the fall season. However, during the spring observational period, currents respond only to a westward component of the wind or to any strong wind of long duration. The strong response to the westward component of the wind may be attributed to the westward geostrophic current which reinforces the tendency for a westward baroclinic flow during this period. □

7. ACKNOWLEDGMENTS

The authors express their gratitude to James Johnson, Diane Haslam, Thomas Baumgardner, and Frank Johnson for their diligence in completing the extensive processing of the MESA data and in sending copies to AOML and NODC; to Terry Mauk and Ann Hildebrand for drawing the many illustrations presented in this report; and to Frank Oxley for photographic assistance. We thank Dr. Michael Devine for the numerous helpful discussions relating to the data analysis and Charles Muirhead for his continuous assistance throughout the MESA Project. We especially thank Terry Thompson for the typing of the tables and manuscript. This work was supported by the National Ocean Survey and the Marine Ecosystems Analysis Program of the National Oceanic and Atmospheric Administration. □

8. REFERENCES

Charnell, R.L., and Hansen, D.V. (1974), *Summary and analysis of physical oceanography data collected in the New York Bight Apex, MESA Report No. 74-3,* 44 pp.

Charnell, R.L., and Mayer, D.A. (1975), *Water movement within the apex of the New York Bight during the summer and fall of 1973, NOAA Technical Memorandum ERL MESA-3,* 32 pp.

Defant, A. (1961), *Physical Oceanography,* Vol. 2, Pergamon Press, New York, N.Y., 598 pp.

Doodson, A.T., and Warburg, H.D. (1941), *Admiralty Manual of Tides,* His Majesty's Stationery Office, London, England, 270 pp.

Groves, G.W. (1955), *Numerical filters for discrimination against tidal periodicities, Transactions, American Geophysical Union,* 36 (6): 1073-1084.

Haight, F.J. (1936), *A rotary wind current off the Florida coast, The Geophysical Review,* 26 (3): 485-488.

Hazelworth, J.B., B.L. Kolitz, R.B. Starr, R.L. Charnell, G.A. Berberian, and M.A. Weiselberg (1975), *New York Bight Project, water column sampling cruises #6-8 of the NOAA ship FERREL, April-June 1974, NOAA Data Report MESA-1,* 177 pp.

Schureman, P. (1958), *Manual of Harmonic Analysis and Prediction of Tides,* U.S. Coast and Geodetic Survey, Special Publication No. 98, rev. ed. (1940), Govt. Printing Office, Washington, D.C., 317 pp.

Swanson, R.L. (1971), *Some aspects of currents in Long Island Sound, Ph.D. Thesis,* Oregon State University, Corvallis, Oregon, 86 pp.

APPENDIX

Definitions of tidal constituents used in this report.

M2 — Principal lunar semidiurnal constituent. This constituent represents the rotation of the Earth with respect to the Moon.

M4, M6, M8 — Shallow water overtides of the principal lunar constituent. The terms take into account the change of M2 tidal wave resulting from shallow water conditions.

S2 — Principal solar semidiurnal constituent. This constituent represents the rotation of the Earth with respect to the Sun.

S4, S6 — Shallow water overtides of the principal solar constituent.

N2 — Larger lunar elliptic semidiurnal constituent. This constituent, with L2, modulates the amplitude and frequency of M2 for the effect of the variation in the Moon's orbital speed caused by its elliptical orbit.

K1 — Lunisolar diurnal constituent. This constituent, with 01, expresses the effect of the Moon's declination. They account for diurnal inequalities and for extreme diurnal tides.

★ U.S. Government Printing Office:1976-680-179